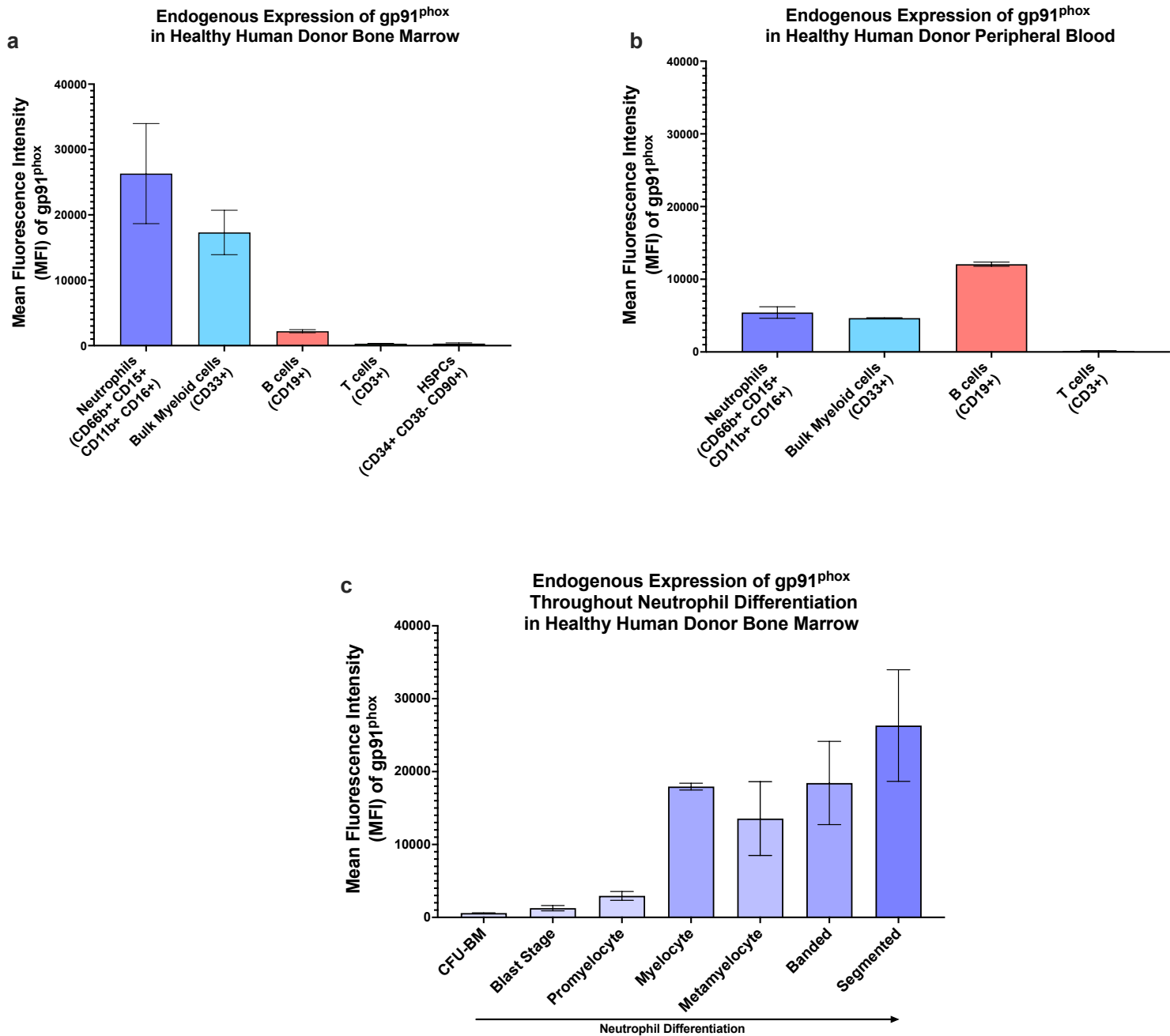
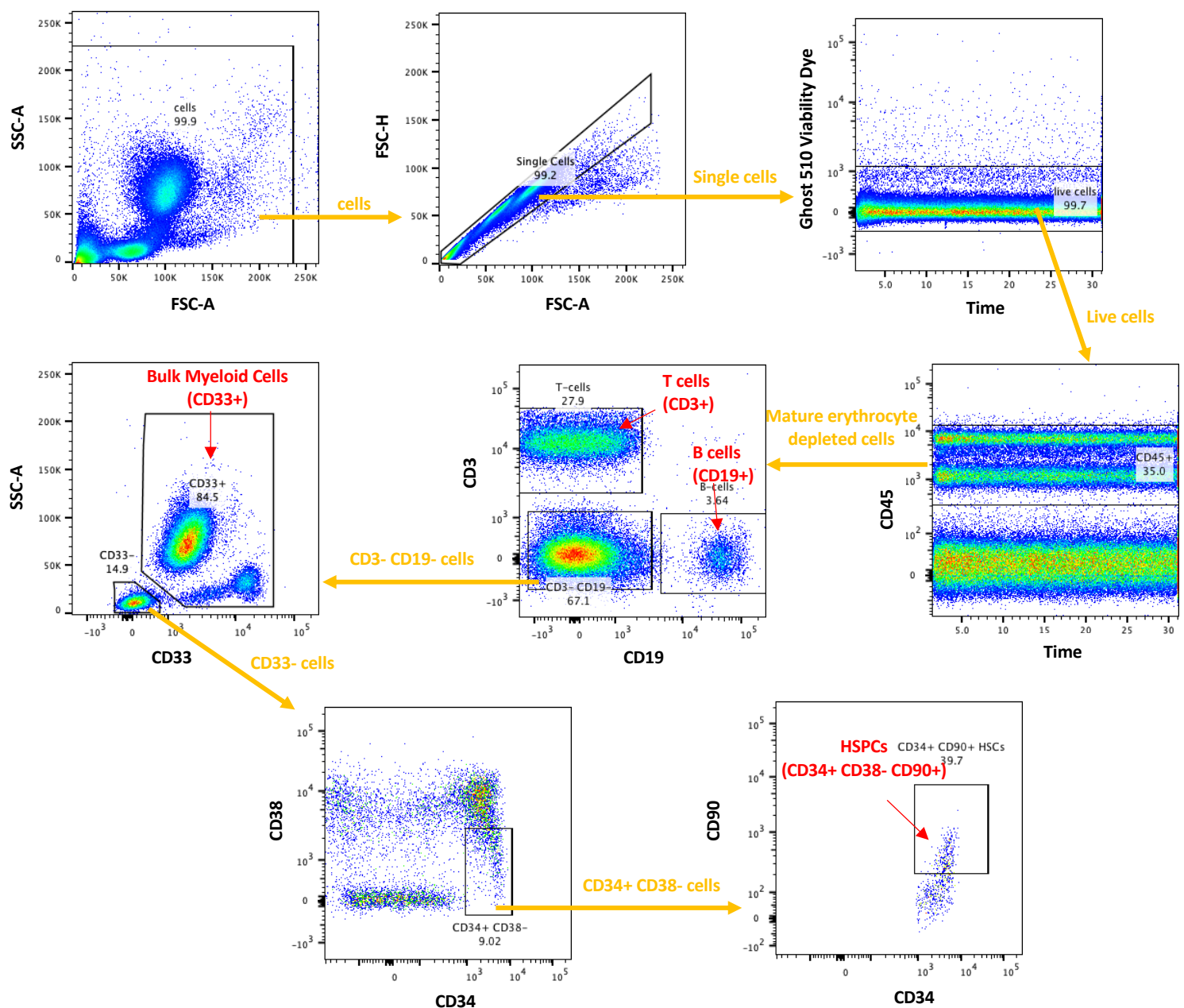


Sup Fig 1) Endogenous expression pattern of gp91^{phox} in healthy human donors and initial analysis of putative regulatory elements within the intronic regions of the CYBB gene and 5000 bp upstream of the CYBB promoter



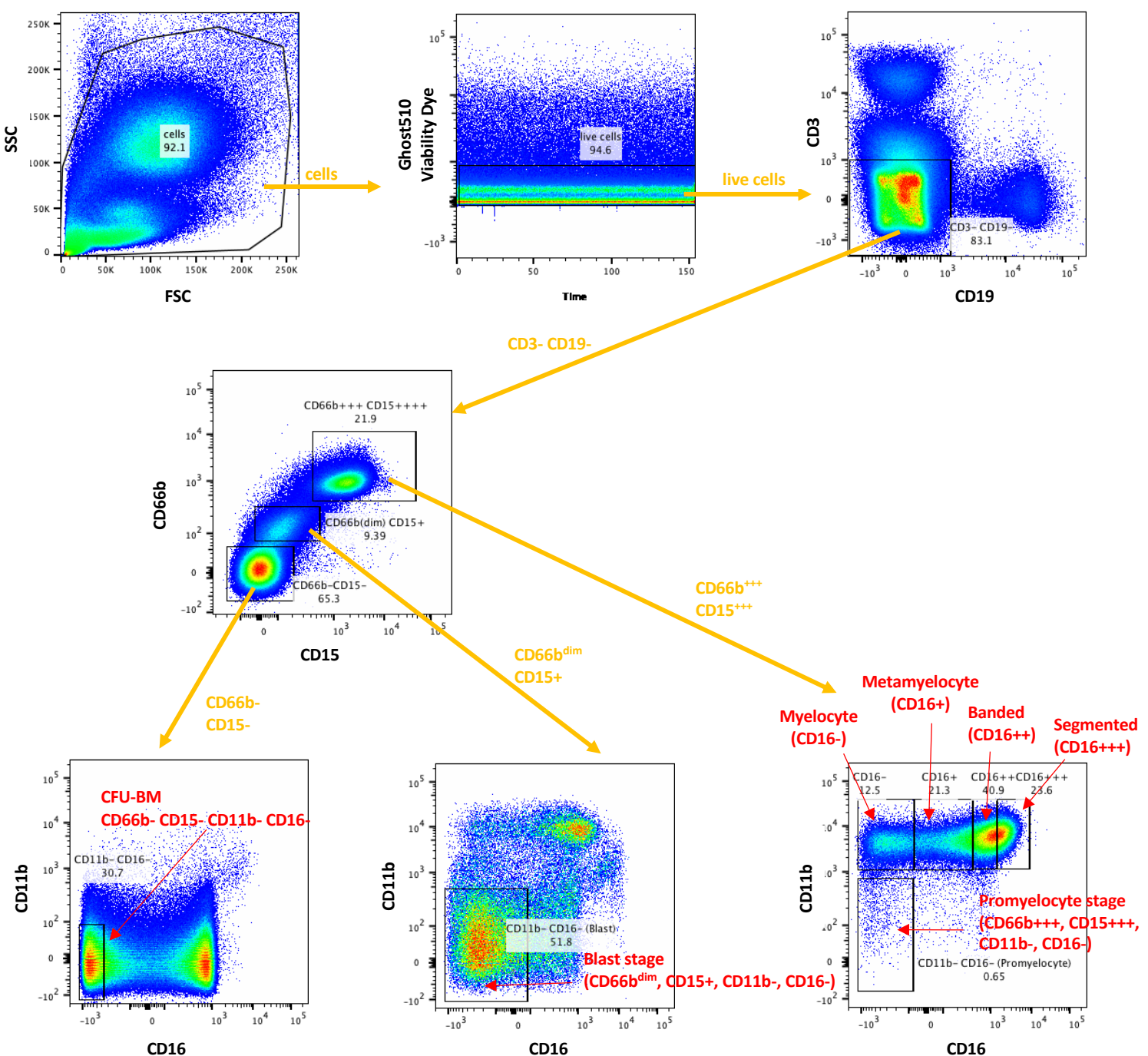
Sup Fig 1) Endogenous expression pattern of gp91^{phox} in healthy human donors and initial analysis of putative regulatory elements within the intronic regions of the CYBB gene and 5000 bp upstream of the CYBB promoter

d

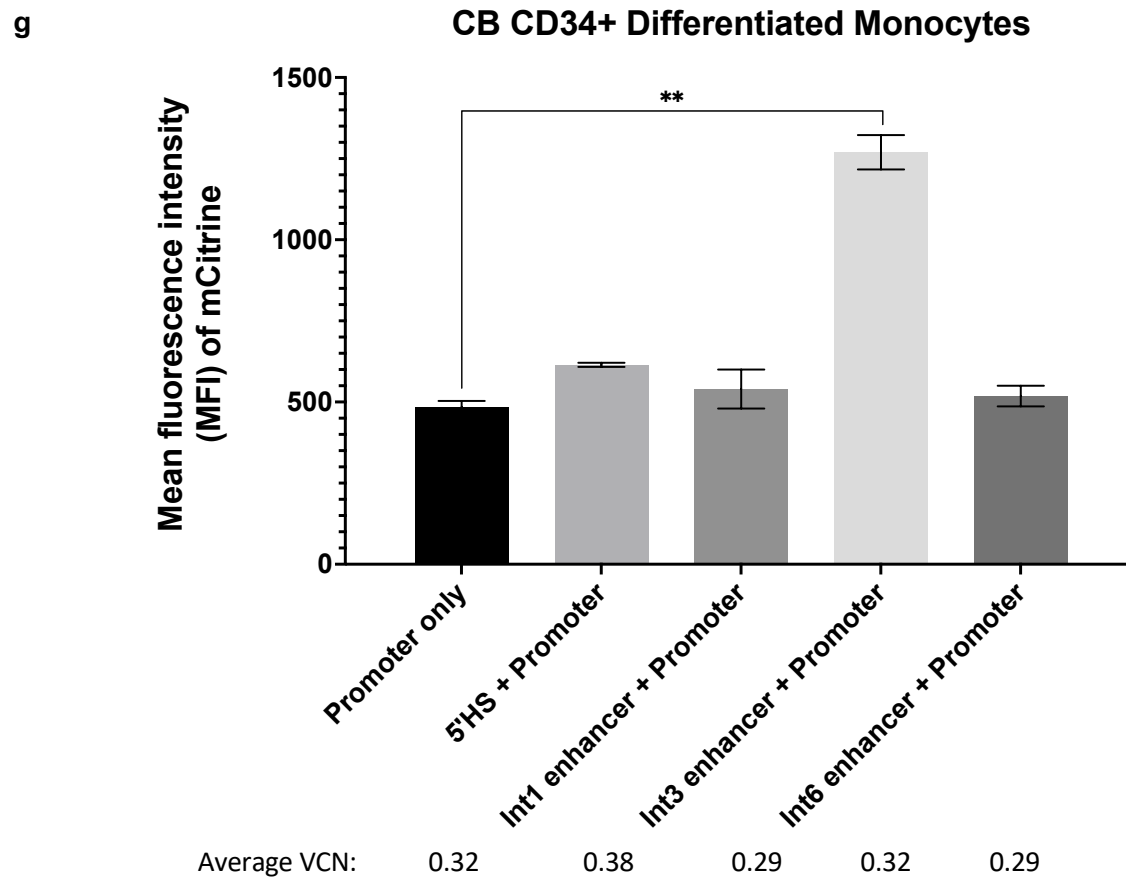
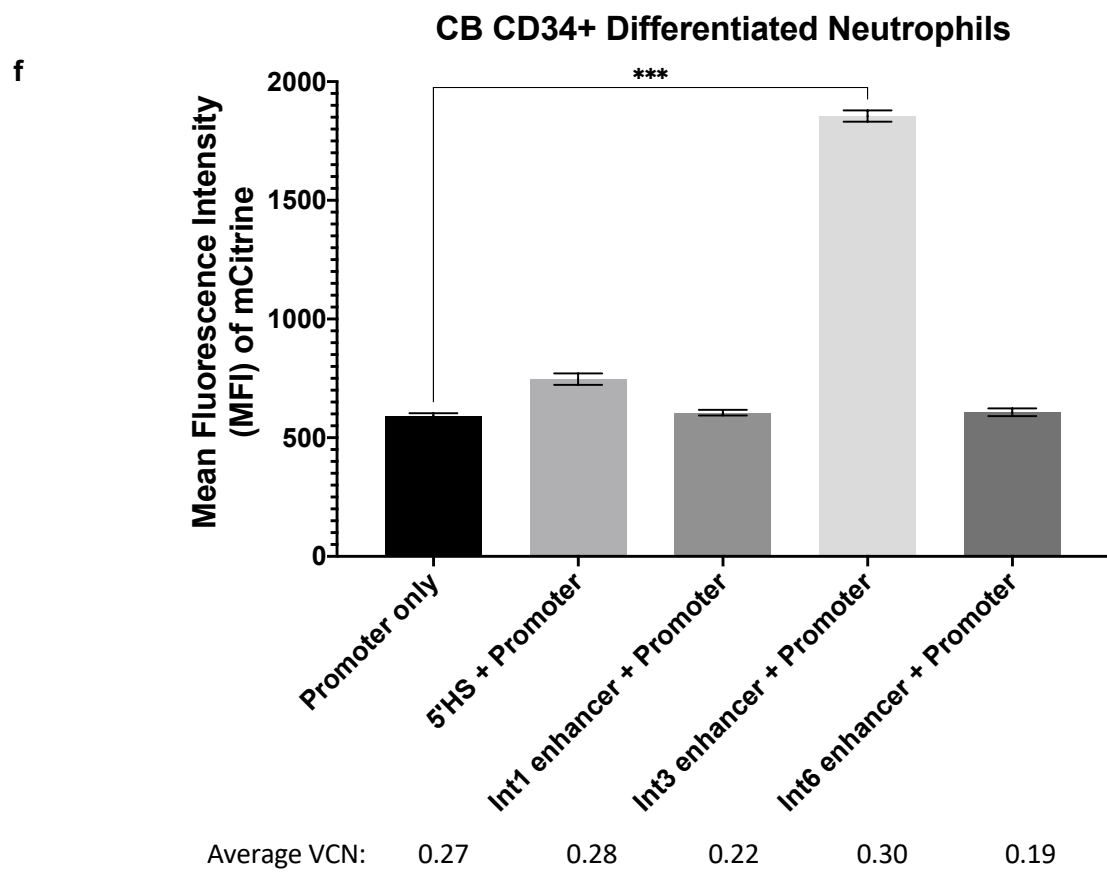


Sup Fig 1) Endogenous expression pattern of gp91^{phox} in healthy human donors and initial analysis of putative regulatory elements within the intronic regions of the CYBB gene and 5000 bp upstream of the CYBB promoter

e

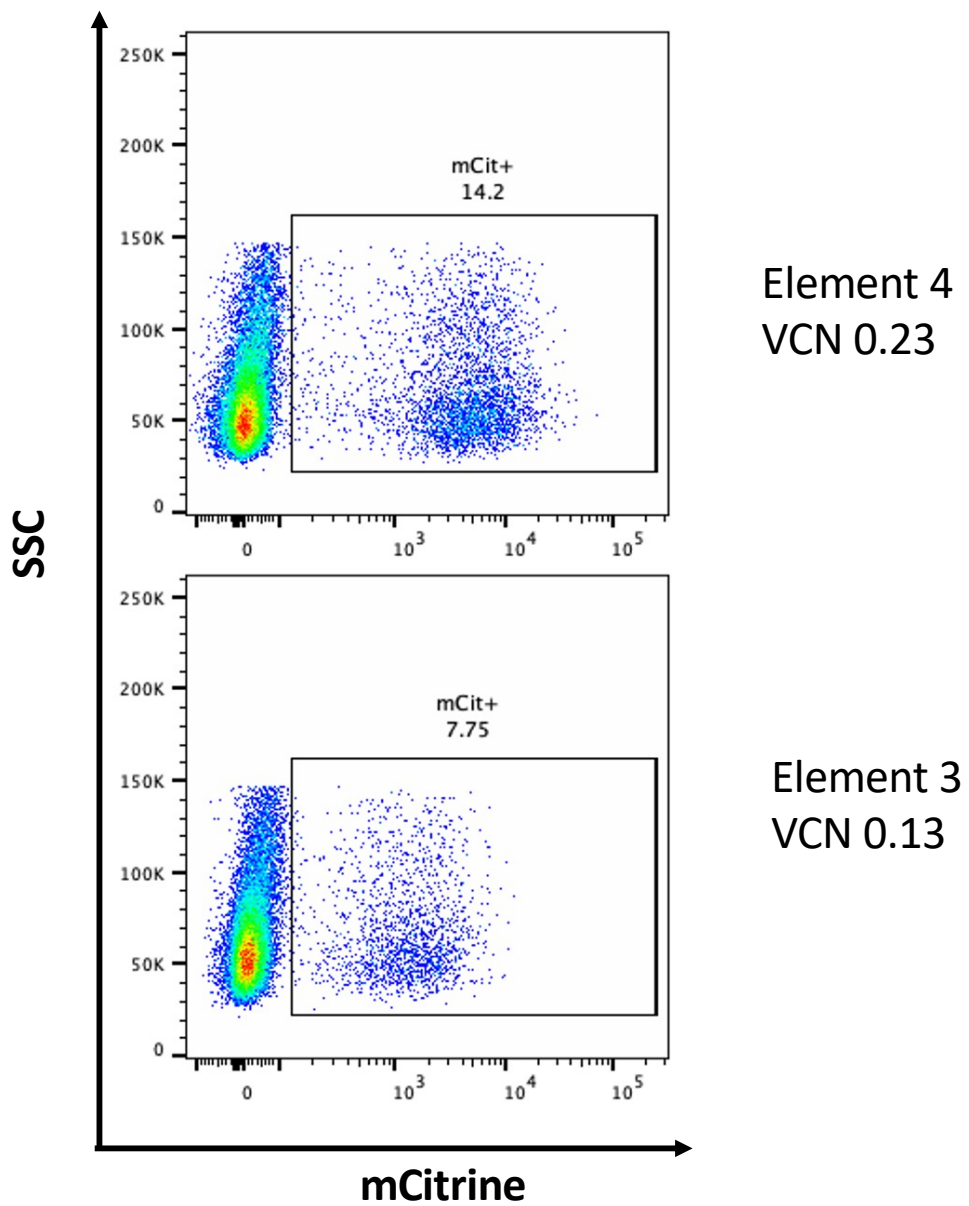


Sup Fig 1) Endogenous expression pattern of gp91^{phox} in healthy human donors and initial analysis of putative regulatory elements within the intronic regions of the CYBB gene and 5000 bp upstream of the CYBB promoter



Sup Fig 1) Endogenous expression pattern of gp91^{phox} in healthy human donors and initial analysis of putative regulatory elements within the intronic regions of the CYBB gene and 5000 bp upstream of the CYBB promoter

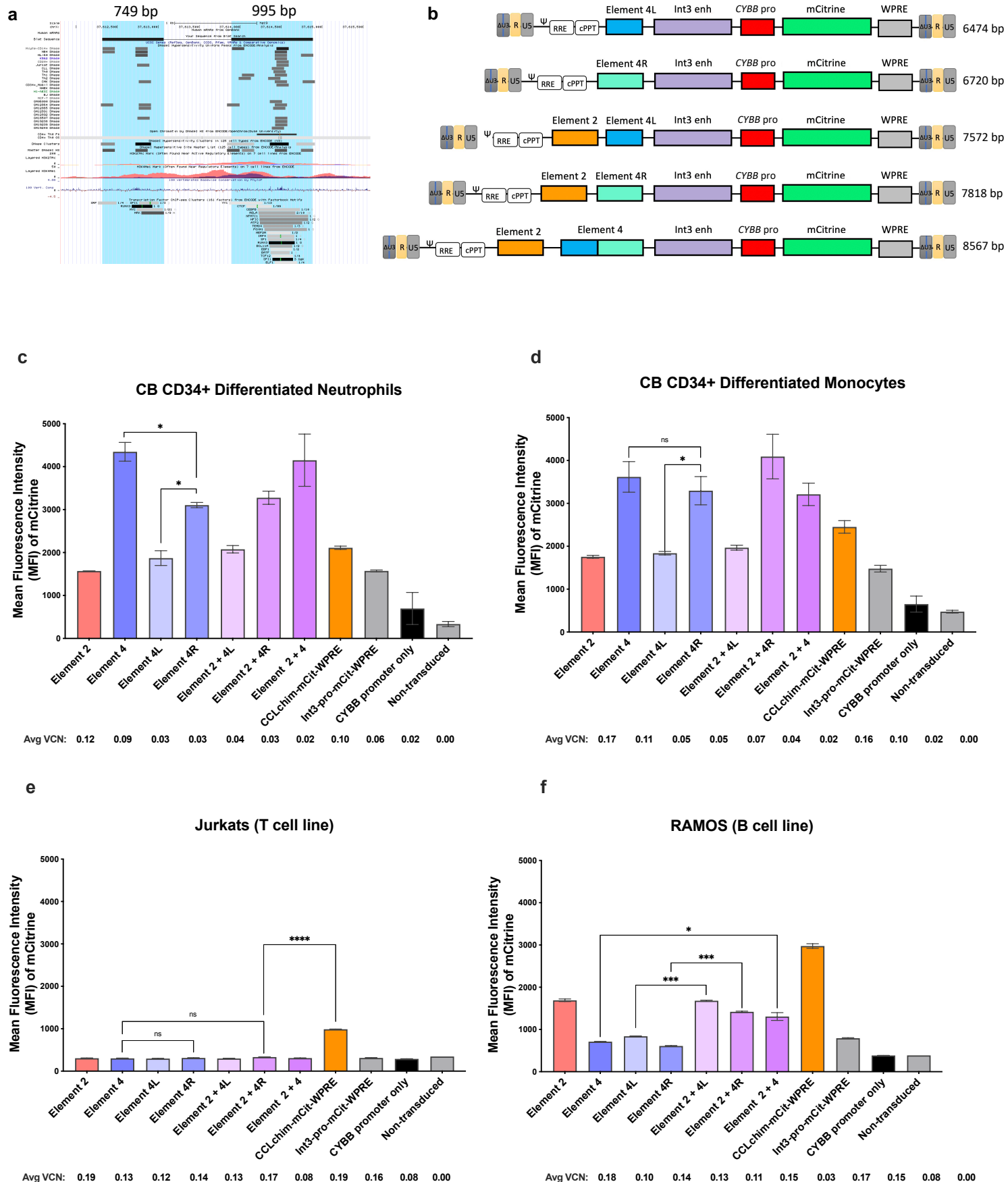
Expression of gp91^{phox} in the (a) bone marrow (BM) and (b) peripheral blood (PB) of 2 healthy human donors. The 2 BM donors are unrelated to the 2 PB donors. (c) Expression of gp91^{phox} throughout neutrophil maturation in the bone marrow. Mean fluorescent intensity (MFI) of gp91^{phox} in each lineage is shown. Data are presented as mean ± SD. Flow gating strategy used to evaluate levels of gp91^{phox} across the (d) different hematopoietic lineages and (e) the different stages of neutrophil differentiation. (f/g) A series of LVs were created, each with a single putative enhancer sequence placed upstream of the CYBB promoter to drive expression of an mCitrine reporter gene. The LVs were transduced into HD CB CD34+ HSPCs and *in vitro* differentiated into mature neutrophils (f) and monocytes (g). MFI of the mCitrine-positive population is shown. (5'HS = 5' Hypersensitive site, Int1 = Intron 1, Int3 = Intron 3, Int6 = Intron 6). Data are presented as mean ± SD. Statistical significance was analyzed using an unpaired t-test. All statistical tests were two-tailed and a p value of < 0.05 was deemed significant (ns non-significant, *P < 0.05, **P < 0.01, ***P < 0.001, ****P < 0.0001.)



Sup Fig 2) Representative flow cytometry plots of the myeloid specific enhancer (element 4) in CD34+ differentiated neutrophils shown in Fig 1c.

Flow cytometry plots demonstrate that the number of vector integrations per cell adhere to a Poisson distribution. The VCN of element 4 is nearly double that of element 3 (VCN of 0.24 vs 0.13, respectively), however, the higher VCN led to a higher number of mCit⁺ cells rather than increasing the amount of integrations per cell. Since we are taking the MFI of the mCit⁺ population in Figure 1 c-f, having more cells in mCit⁺ population does not affect the MFI.

Sup Fig 3) Designing the composite X-CGD vector containing the key endogenous regulatory elements

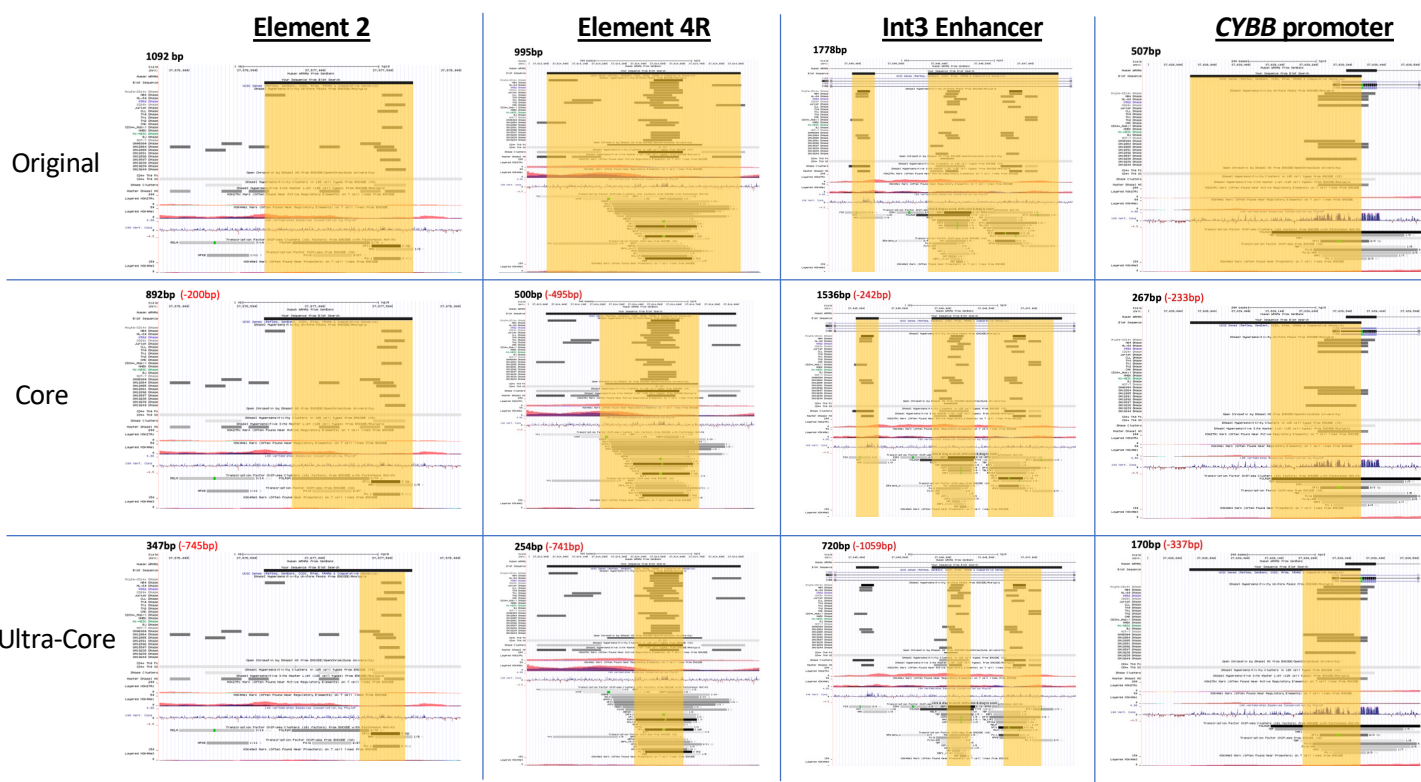


Sup Fig 3) Designing the composite X-CGD vector containing the critical endogenous regulatory elements

(a) Visual representation of element 4 in the UCSC Genome Browser. The 749bp left and 995bp right fragments are highlighted in blue. (b) A series of LVs were designed to determine the critical fragment within element 4 as well as a series of composite vectors to be potential lead candidates. Results of the enhancer screen in CB CD34+ differentiated (c) neutrophils and (d) monocytes, (e) Jurkats and (f) RAMOs cell lines. MFI of the mCitrine positive population is shown. (4L = left fragment of element 4, 4R = right fragment of element 4, Int3 = *CYBB* intron 3 enhancer, mCit = mCitrine, pro = *CYBB* promoter, WPRE = Woodchuck Hepatitis Virus Posttranscriptional Regulatory Element). Data are presented as mean \pm SD. Statistical significance was analyzed using an unpaired t-test. All statistical tests were two-tailed and a p value of < 0.05 was deemed significant (ns non-significant, * $P < 0.05$, ** $P < 0.01$, *** $P < 0.001$, **** $P < 0.0001$.)

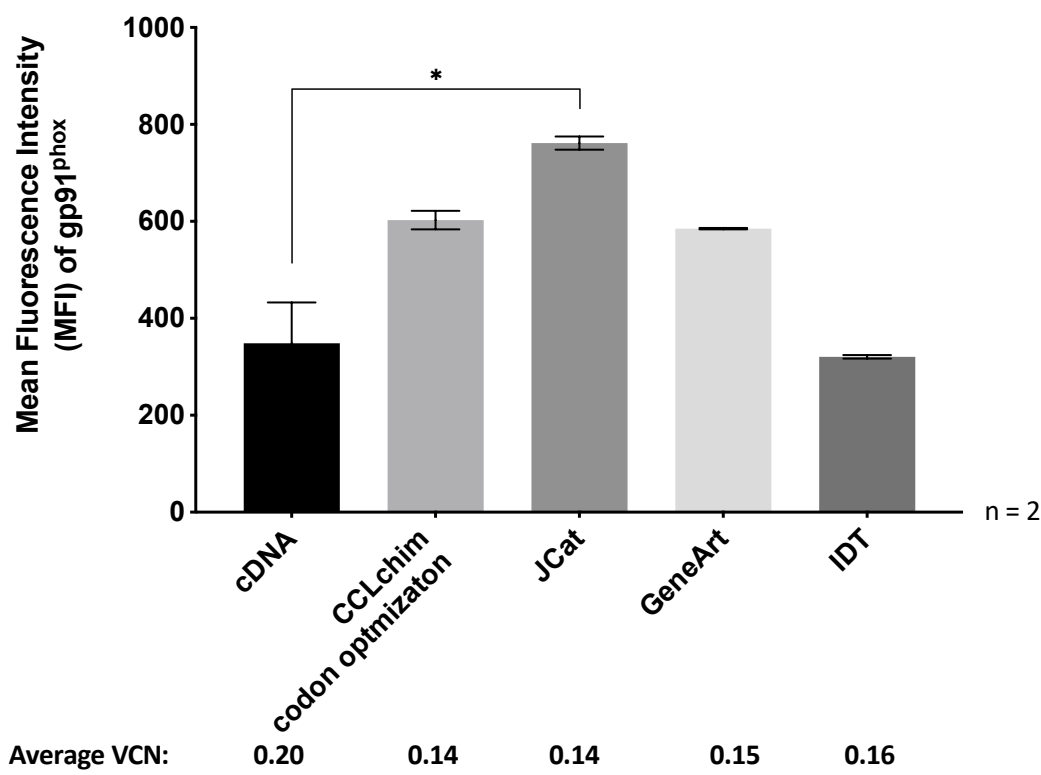
Sup Fig 4) Optimizing the size of the key endogenous elements of the *CYBB* gene and codon optimization of gp91^{phox}

a



b

Codon Optimization of gp91^{phox} in PLB-985 *CYBB*^{-/-} cells

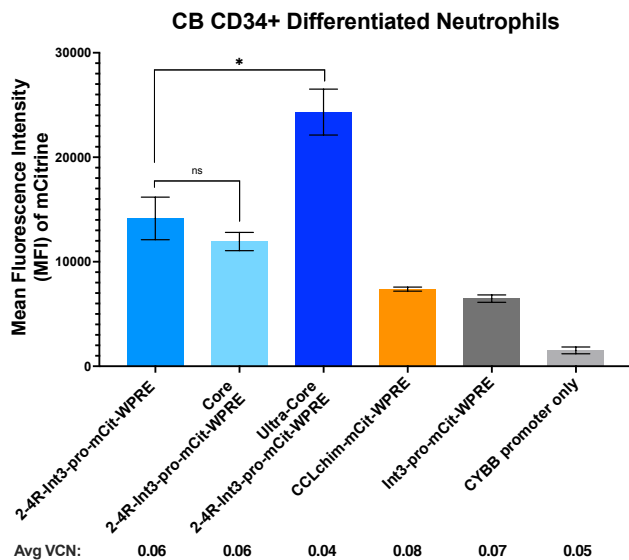


Sup Fig 4) Optimizing the size of the key endogenous elements of the *CYBB* gene and codon optimization of gp91^{phox}

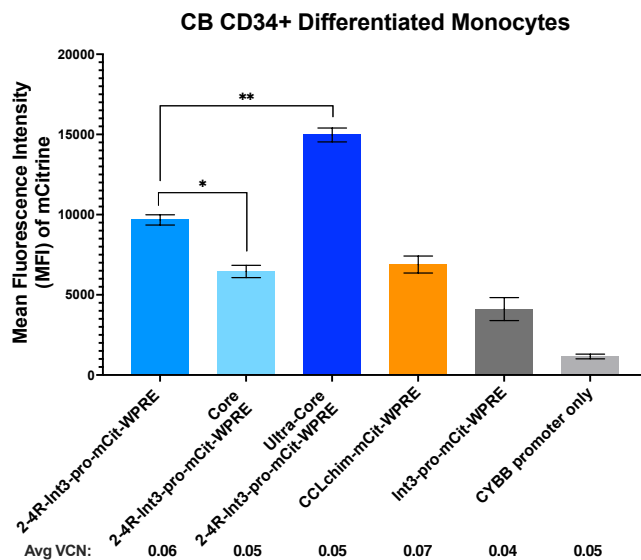
(a) Using ENCODE data, the functional boundaries of the “core” elements were defined by transcription factor binding footprint demarcated by ChIP-Seq. The boundaries of the “ultra-core” elements were defined by lineage specific DNaseI Hypersensitivity. We designed the “core” and “ultra-core” variants using these newly defined enhancer boundaries (highlighted in yellow). (4R = right fragment of element 4, Int3 = *CYBB* intron 3 enhancer) (b) Different codon optimized variants of the gp91^{phox} gene were screened in *CYBB*^{-/-} PLB-985 cells. MFI of the gp91^{phox}-positive population is shown. Data are presented as mean ± SD. Statistical significance was analyzed using an unpaired t-test. All statistical tests were two-tailed and a p value of < 0.05 was deemed significant (ns non-significant, *P < 0.05, **P < 0.01, ***P < 0.001, ****P < 0.0001.)

Sup Fig 5) Generation of the lead candidate vector with improved expression, titer and gene transfer

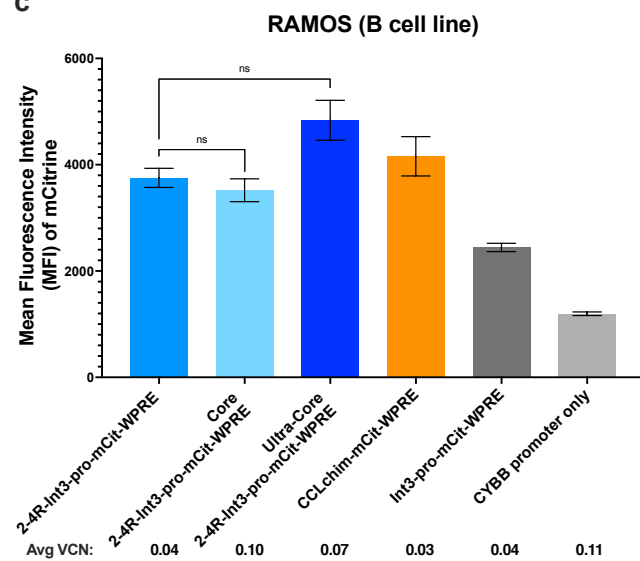
a



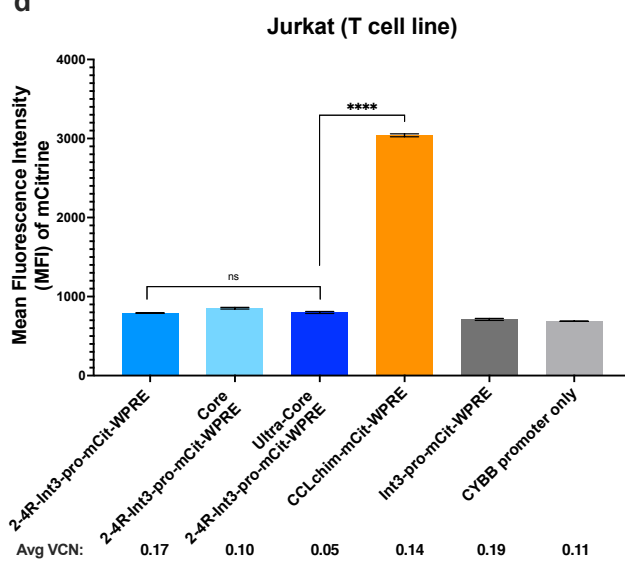
b



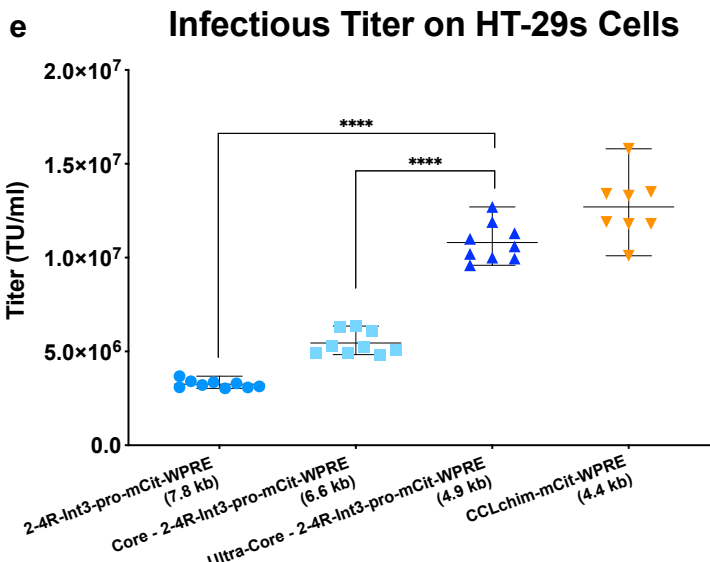
c



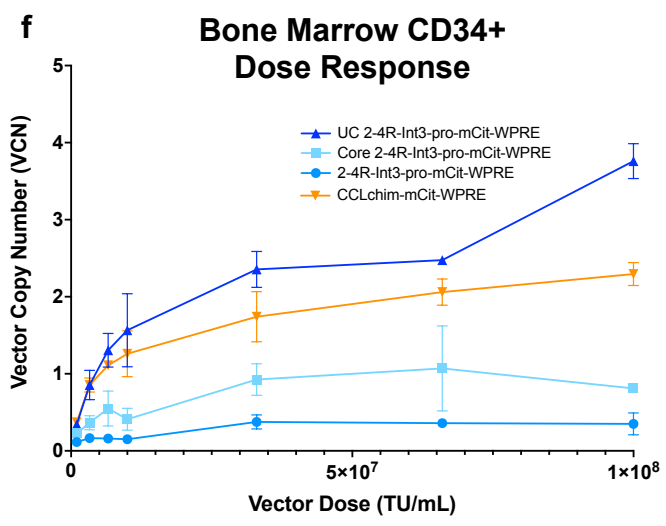
d



e



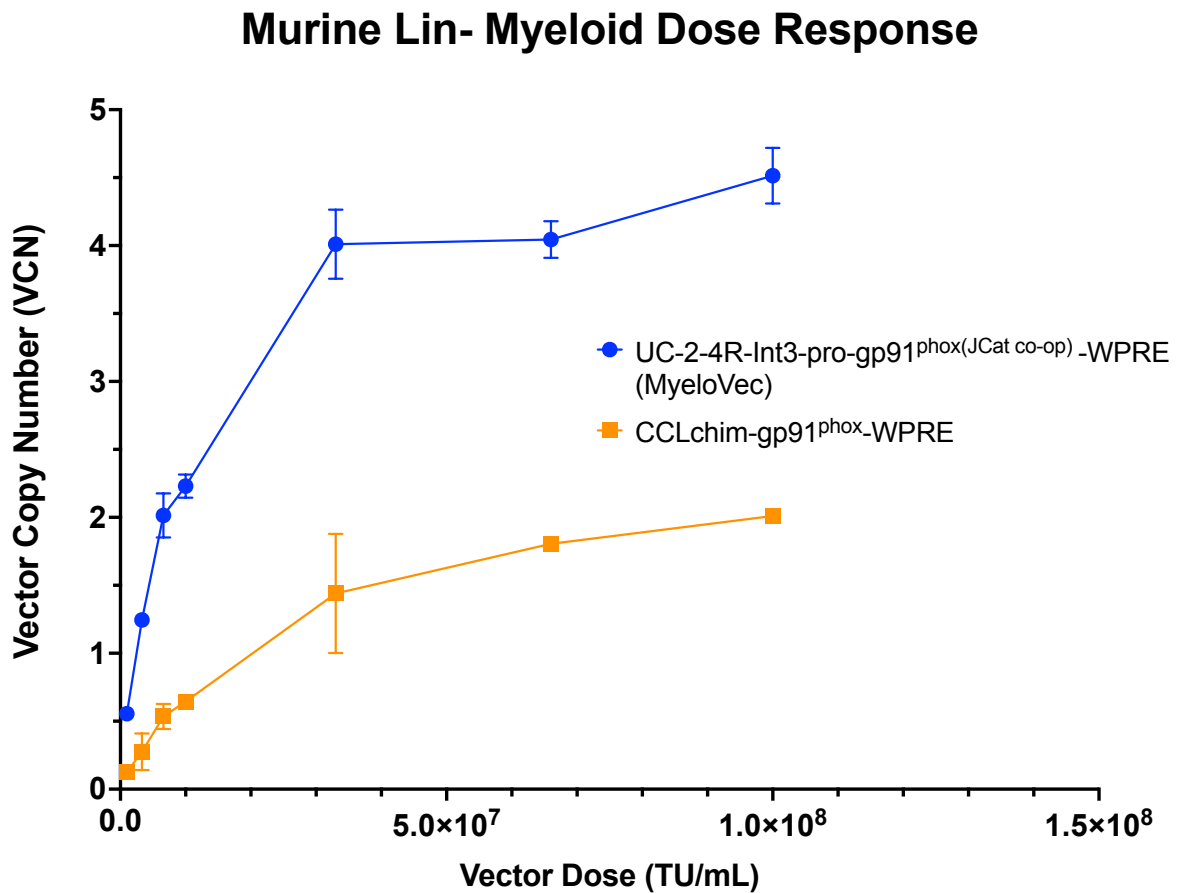
f



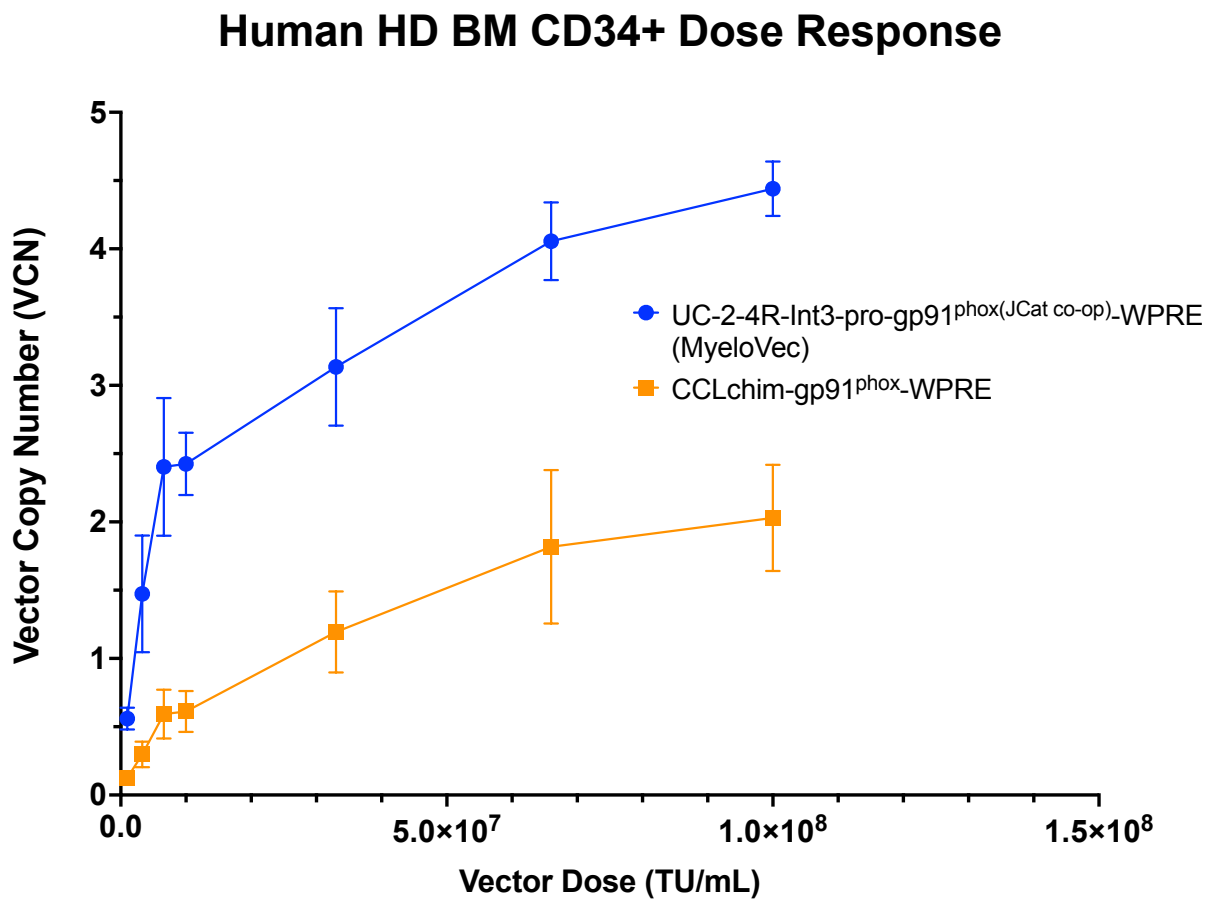
Sup Fig 5) Generation of the lead candidate vector with improved expression, titer and gene transfer

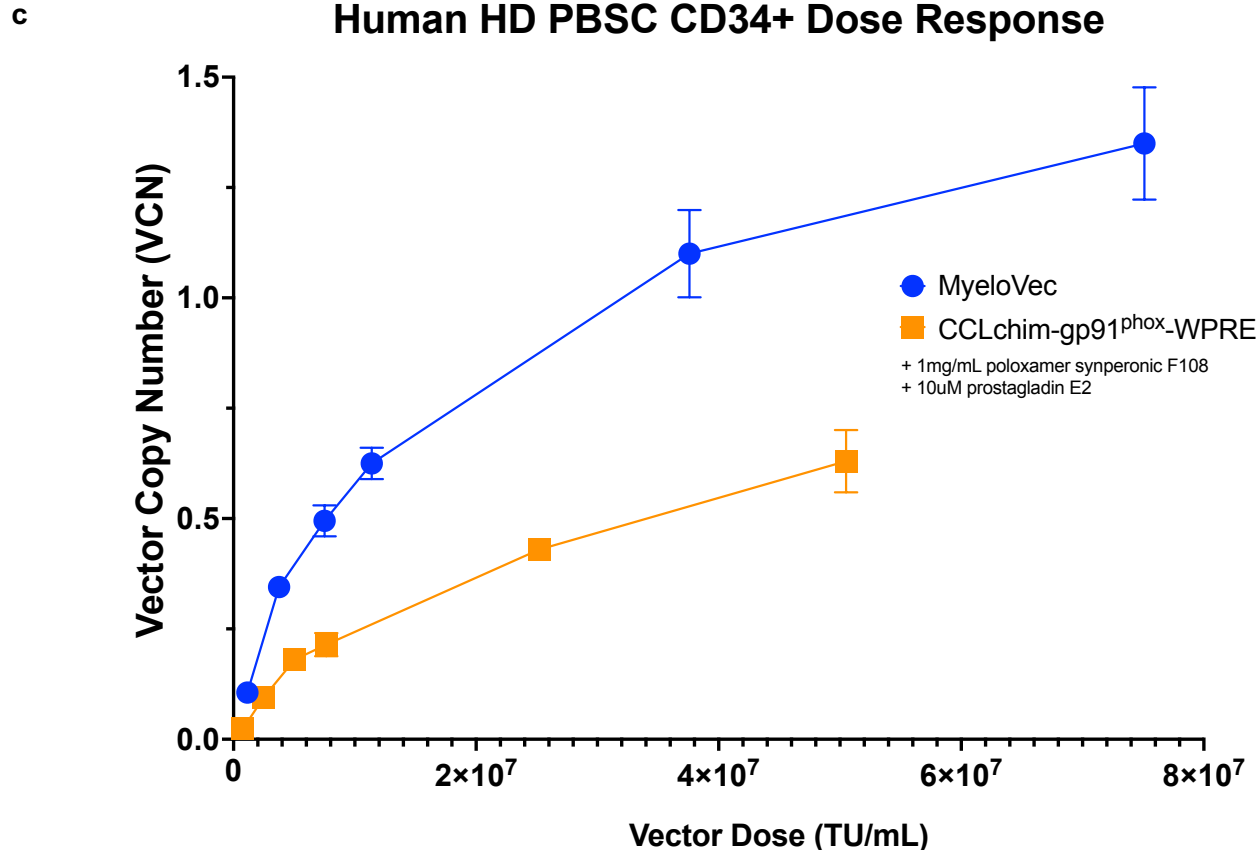
MFI of the mCitrine-positive population is shown in CB CD34+ differentiated (a) neutrophils and (b) monocytes and in (c) RAMOs and (d) Jurkat cell lines. (e) Raw unconcentrated viral supernatant of the parental, core and ultra-core variant as well as the pCCLchim vector were titrated on HT-29 cells. (f) Human HD BM CD34+ HPSCs were transduced with increasing doses of concentrated viral supernatant to assess gene transfer. Stable VCN at each dose were measured 14-days post transduction. (4R = right fragment of element 4, Int3 = *CYBB* intron 3 enhancer, mCit = mCitrine, pro = *CYBB* promoter, WPRE = Woodchuck Hepatitis Virus Posttranscriptional Regulatory Element). Data are presented as mean \pm SD. Statistical significance was analyzed using an unpaired t-test. All statistical tests were two-tailed and a p value of < 0.05 was deemed significant (ns non-significant, * $P < 0.05$, ** $P < 0.01$, *** $P < 0.001$, **** $P < 0.0001$.)

a



b

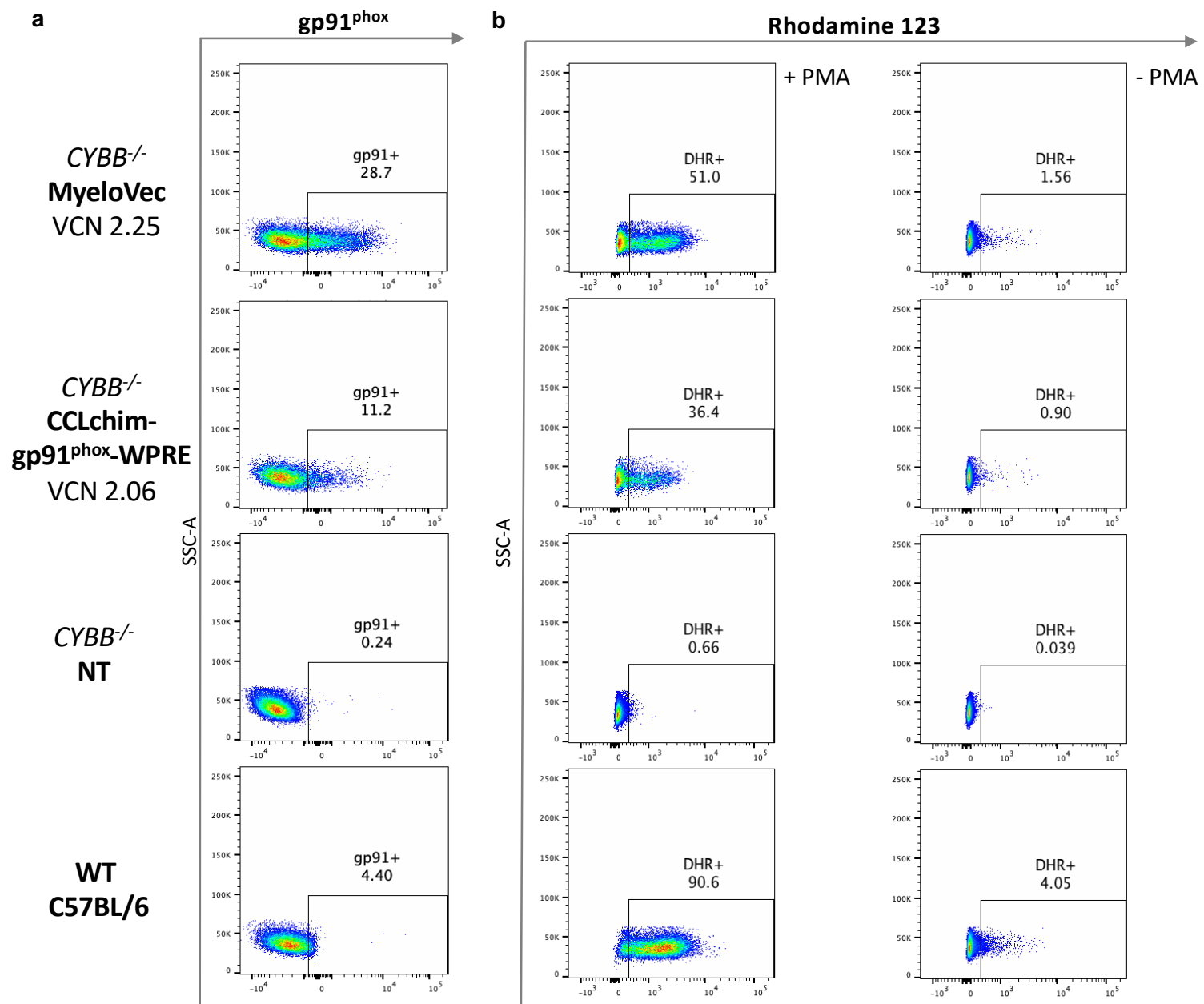




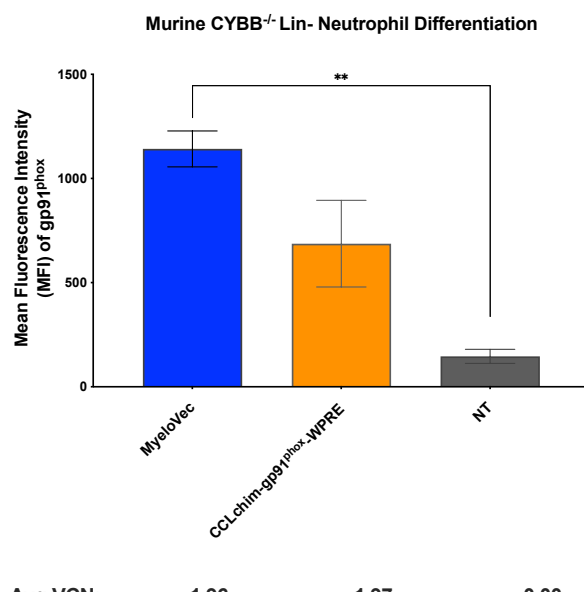
Sup Fig 6) VCN dose response in murine Lin- HSPCs and in human HD HSPCs

(a) Murine Lin- HSPCs, (b) Human HD CD34+ BM HPSCs, or (c) Human HD CD34+ mobilized peripheral blood HSPCs were transduced with increasing doses of MyeloVec (UC-2-4R-Int3-pro-gp91^{phox}-WPRE) or CCLchim-gp91^{phox}-WPRE. Stable VCN was taken after 14 days in culture. Transduction enhancers were used for the donor in (c), known to be less permissive to transduction to show that MyeloVec maintains its gene transfer advantage even in the presence of transduction enhancers.

Sup Fig 7) Correction of X-CGD murine cells *in vitro*



c



d

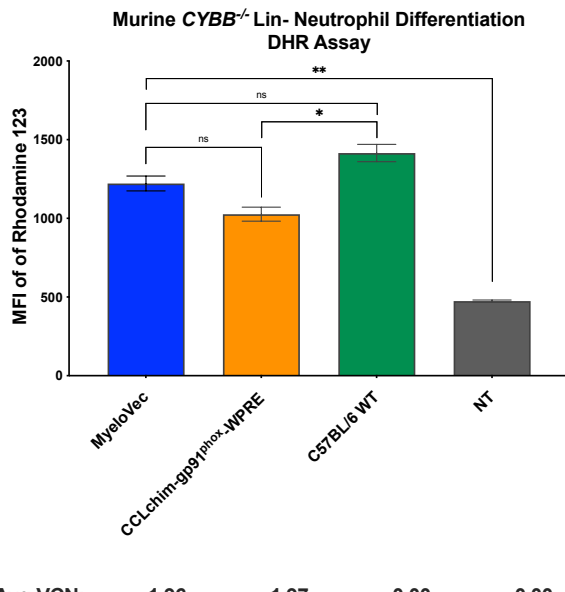
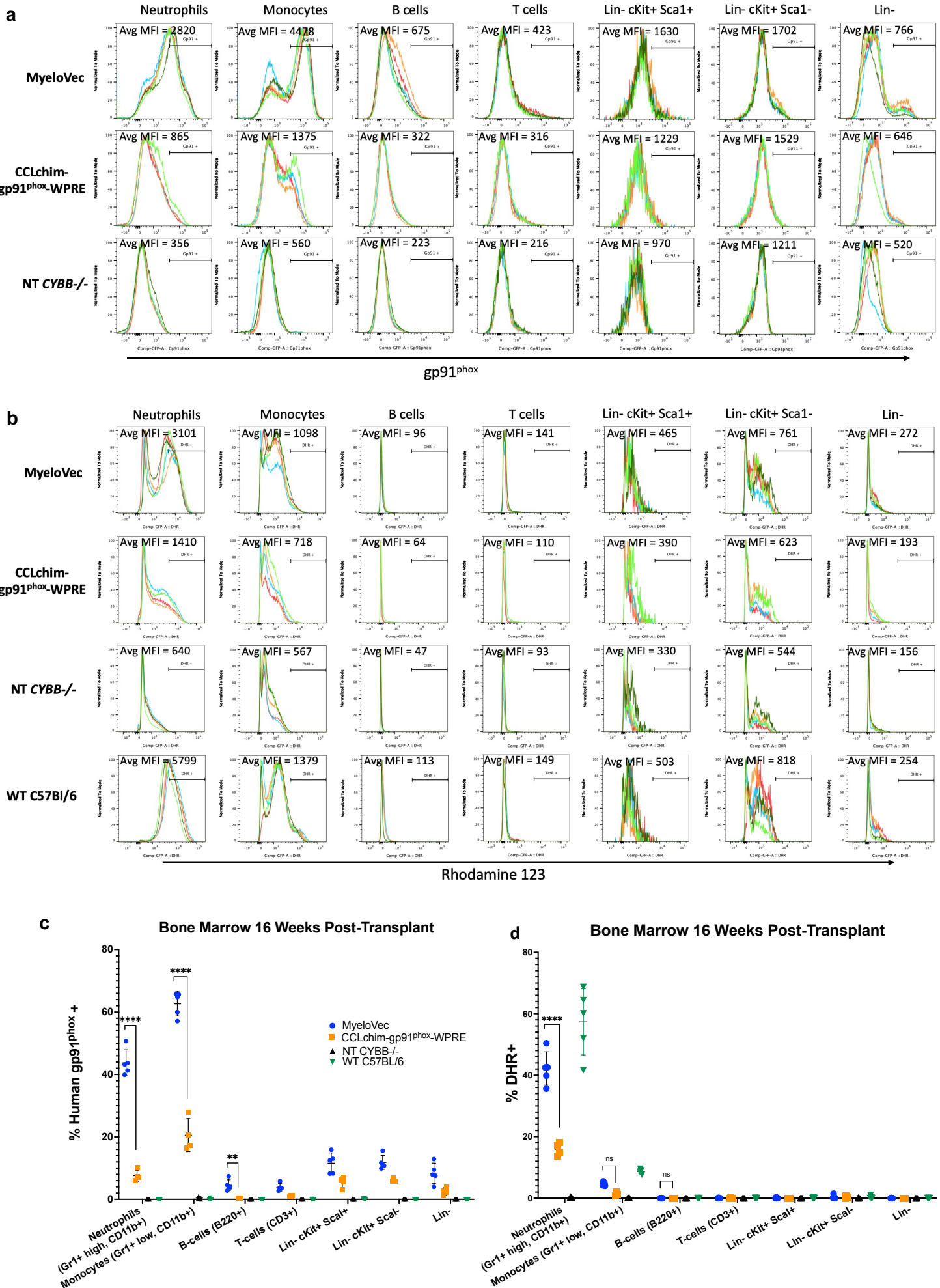


Fig 7) Correction of X-CGD mouse model in vitro

X-CGD murine HSPCs were transduced with MyeloVec or CCLchim vectors expressing gp91^{phox} and differentiated into mature neutrophils. (a) Representative flow cytometry plots exhibit restoration of gp91^{phox} expression. The anti-human gp91^{phox} antibody (7D5 clone) was only able to detect expression of human gp91^{phox} expressed from the vectors but not murine gp91^{phox} from the WT murine cells. MFI of the gp91^{phox}-positive population is shown in panel (c). (b) Flow cytometry plots displaying restoration of functional oxidase activity measured by the DHR flow cytometry. MyeloVec transduced cells restored oxidase activity to wildtype levels. MFI of Rhodamine-positive cells are shown in panel (d). Data are presented as mean ± SD. Statistical significance was analyzed using an unpaired t-test. All statistical tests were two-tailed and a p value of < 0.05 was deemed significant (ns non-significant, *P < 0.05, **P < 0.01, ***P < 0.001, ****P < 0.0001.)

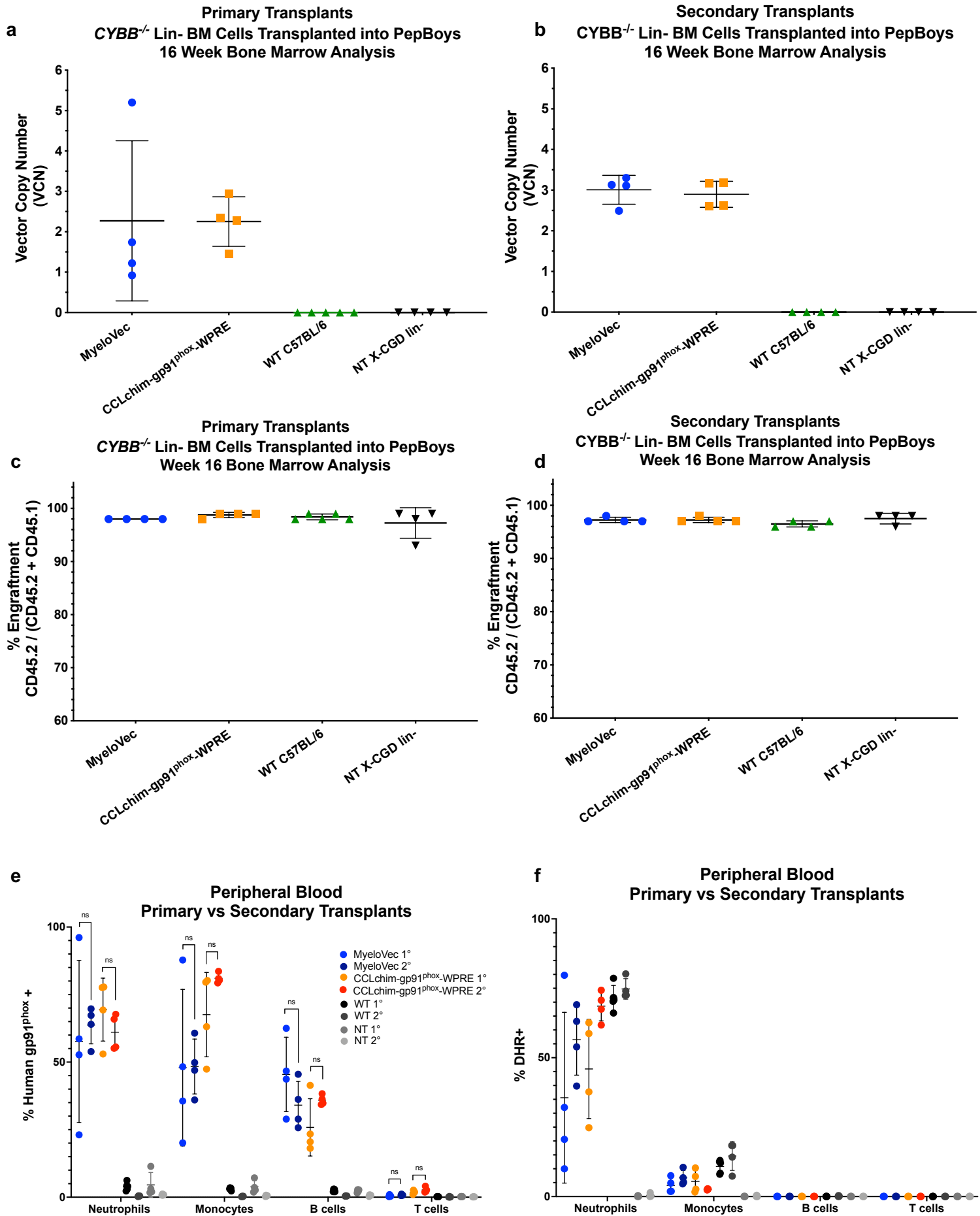
Sup Fig 8) Lineage specific expression of MyeloVec in the BM of transplanted mice

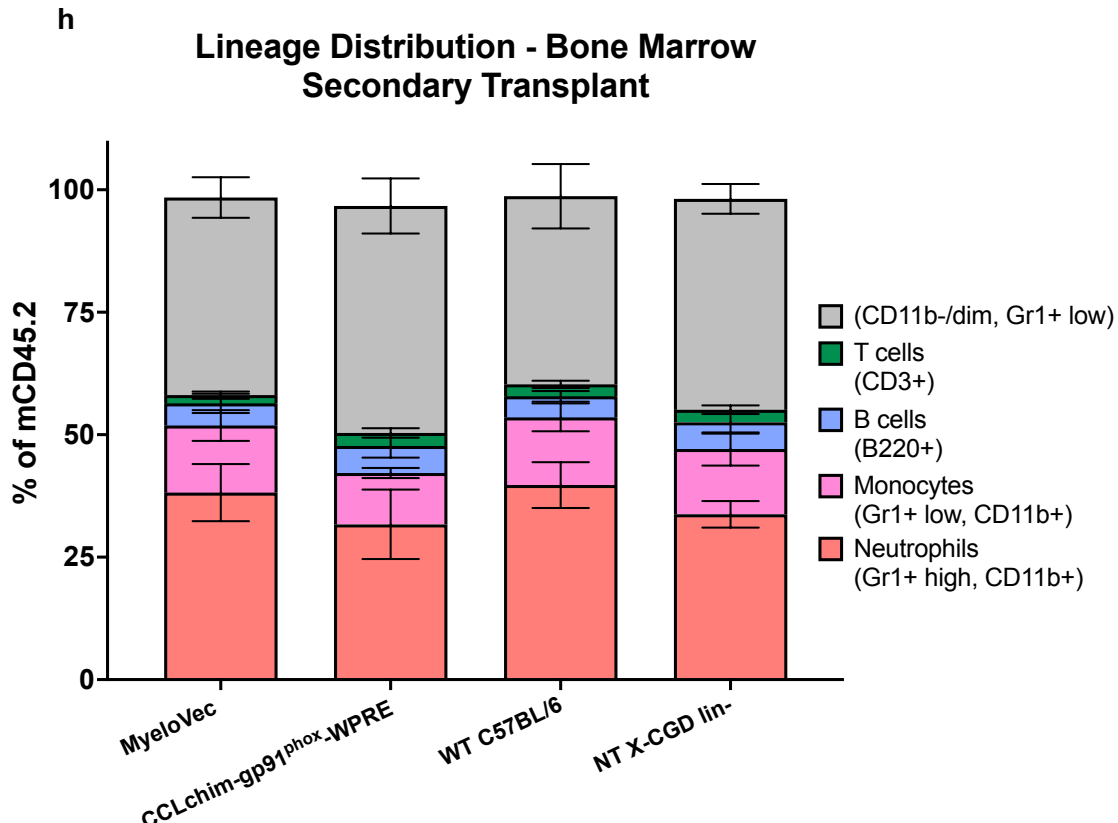
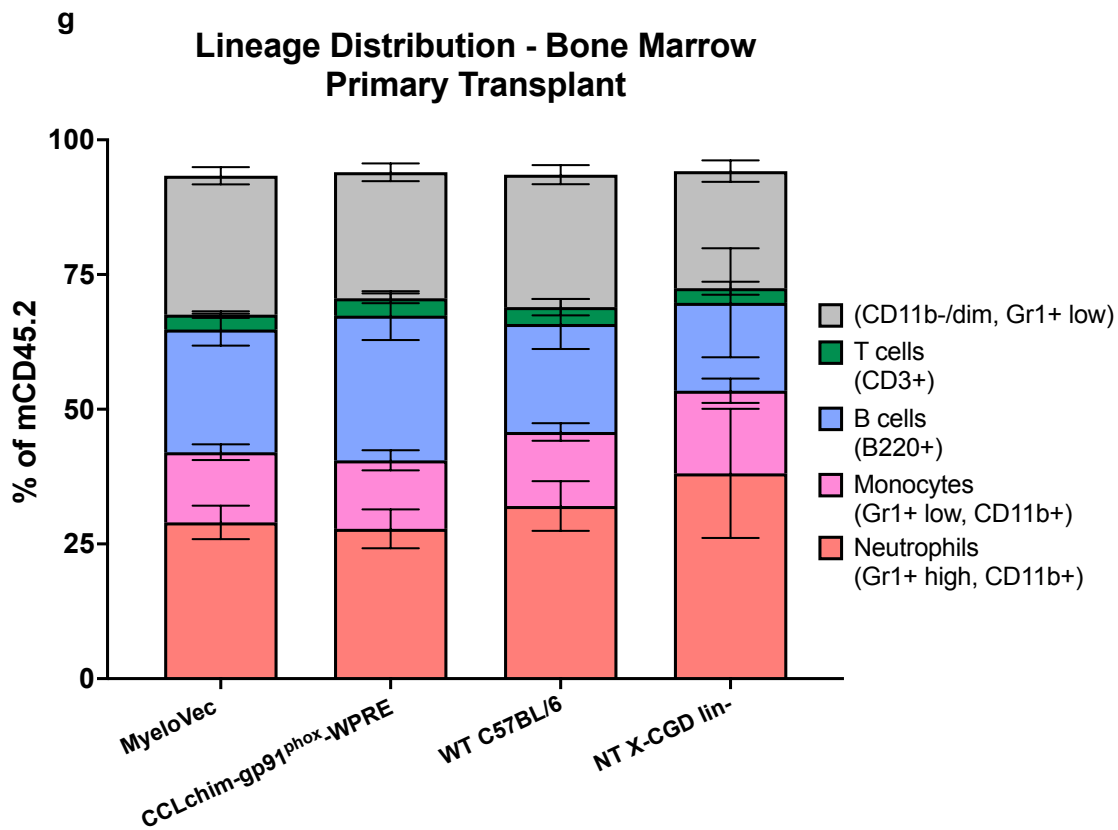


Sup Fig 8) Lineage specific expression of MyeloVec in the BM of transplanted mice

CD45.2 murine X-CGD Lin- HPSCs were transplanted into CD45.1 Pepboy mice (same experiment shown in Figure 5). WT C57BL/6 and NT X-CGD lin- HPSCs were also transplanted as controls. (a,c) Restoration of gp91^{phox} and (b,d) oxidase activity were evaluated across the different hematopoietic lineages in the BM of the mice 16 weeks post-transplant. Data are presented as mean \pm SD. Statistical significance was analyzed using a two-way ANOVA followed by multiple paired comparisons for normally distributed data (Tukey test). All statistical tests were two-tailed and a p value of < 0.05 was deemed significant (ns non-significant, * $P < 0.05$, ** $P < 0.01$, *** $P < 0.001$, **** $P < 0.0001$.)

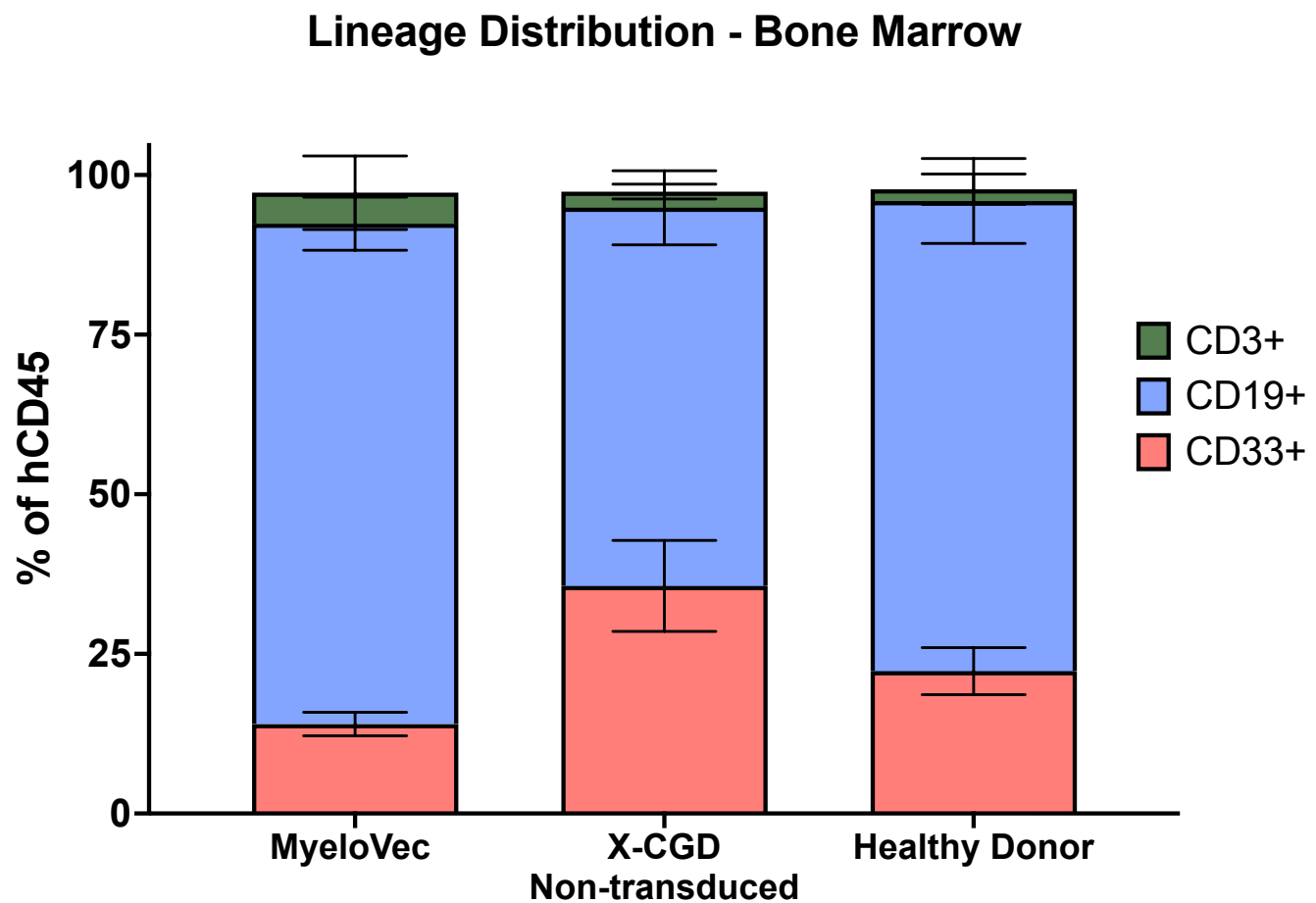
Sup Fig 9) Maintenance of gp91^{phox} expression, oxidase activity and VCN in secondary transplants





Sup Fig 9) Maintenance of gp91^{phox} expression, oxidase activity and VCN in secondary transplants.

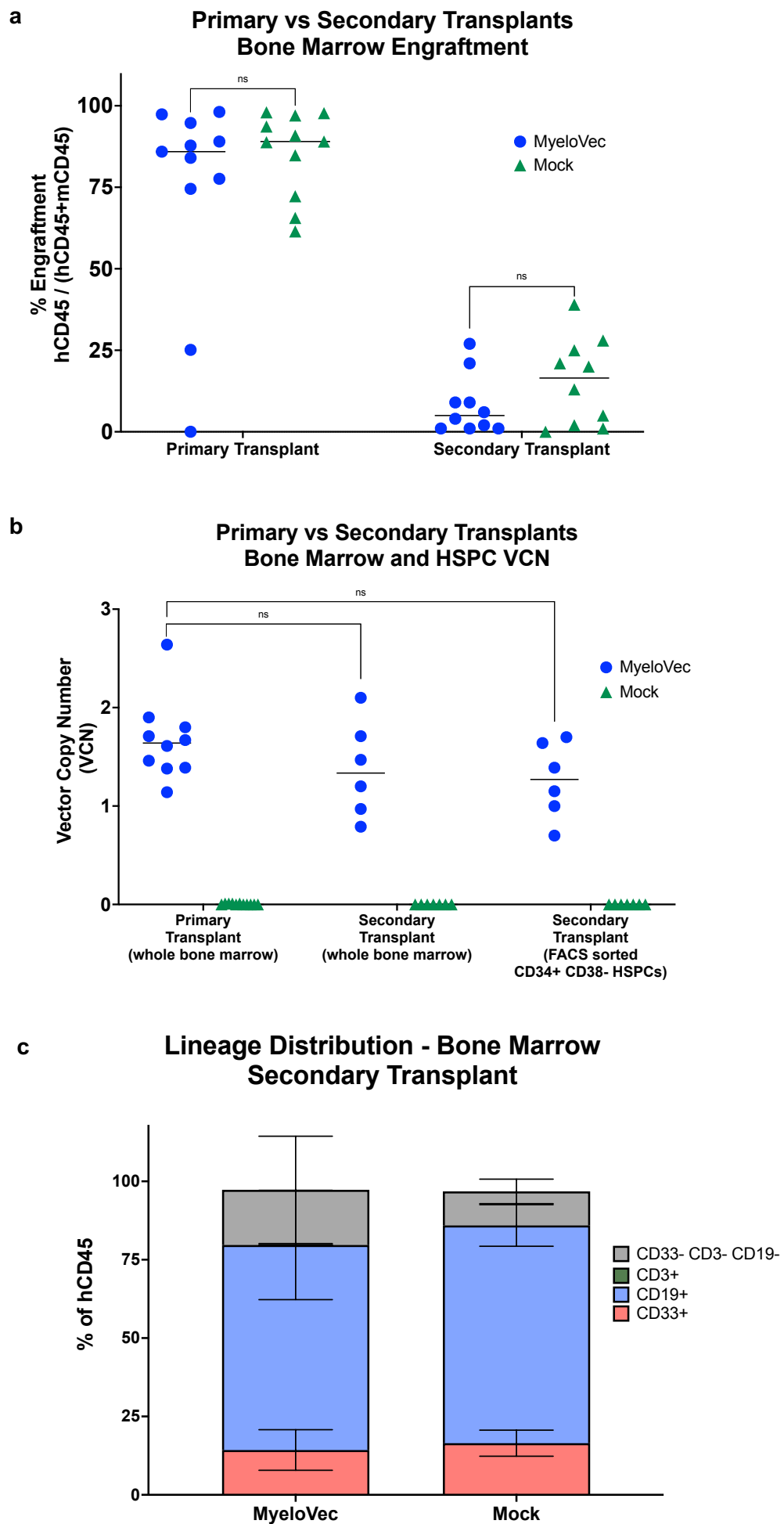
For the primary transplants, lethally irradiated Pepboy mice were engrafted with either MyeloVec or CCLchim transduced murine X-CGD HSPCs. WT C57BL/6 and non-transduced X-CGD HPSCs were also transplanted as positive and negative controls, respectively. The cell products were transduced to produce an equal VCN. Primary mice were harvested 16 weeks post-transplant and whole BM was collected and pooled for each treatment arm. 30e6 whole BM cells were injected into each of the lethally irradiated secondary Pepboy recipients. Secondary transplanted mice were harvest after an additional 16 weeks. BM VCN and engraftment of the (a/c) primary and (b/d) secondary mice. Percent (e) gp91^{phox}-positive and (f) oxidase-positive cells across the different lineages were maintained between the primary and secondary transplants. Lineage distribution of the engrafted CD45.2 cells in the (g) primary and (h) secondary transplanted mice. Data are presented as mean ± SD. Statistical significance was analyzed using a two-way ANOVA followed by multiple paired comparisons for normally distributed data (Tukey test). All statistical tests were two-tailed and a p value of < 0.05 was deemed significant (ns non-significant, *P < 0.05, **P < 0.01, ***P < 0.001, ****P < 0.0001.)



Sup Fig 10) Lineage distribution of reconstituted X-CGD patient cells in NSG bone marrow

NSG neonatal mice transplanted with X-CGD patient HSPCs were harvested 16-weeks post-transplant and lineage distribution of engrafted human cells was analyzed by flow cytometry.

Sup Fig 11) Preservation of MyeloVec Transduced HSPCs in Secondary NBSGW mice

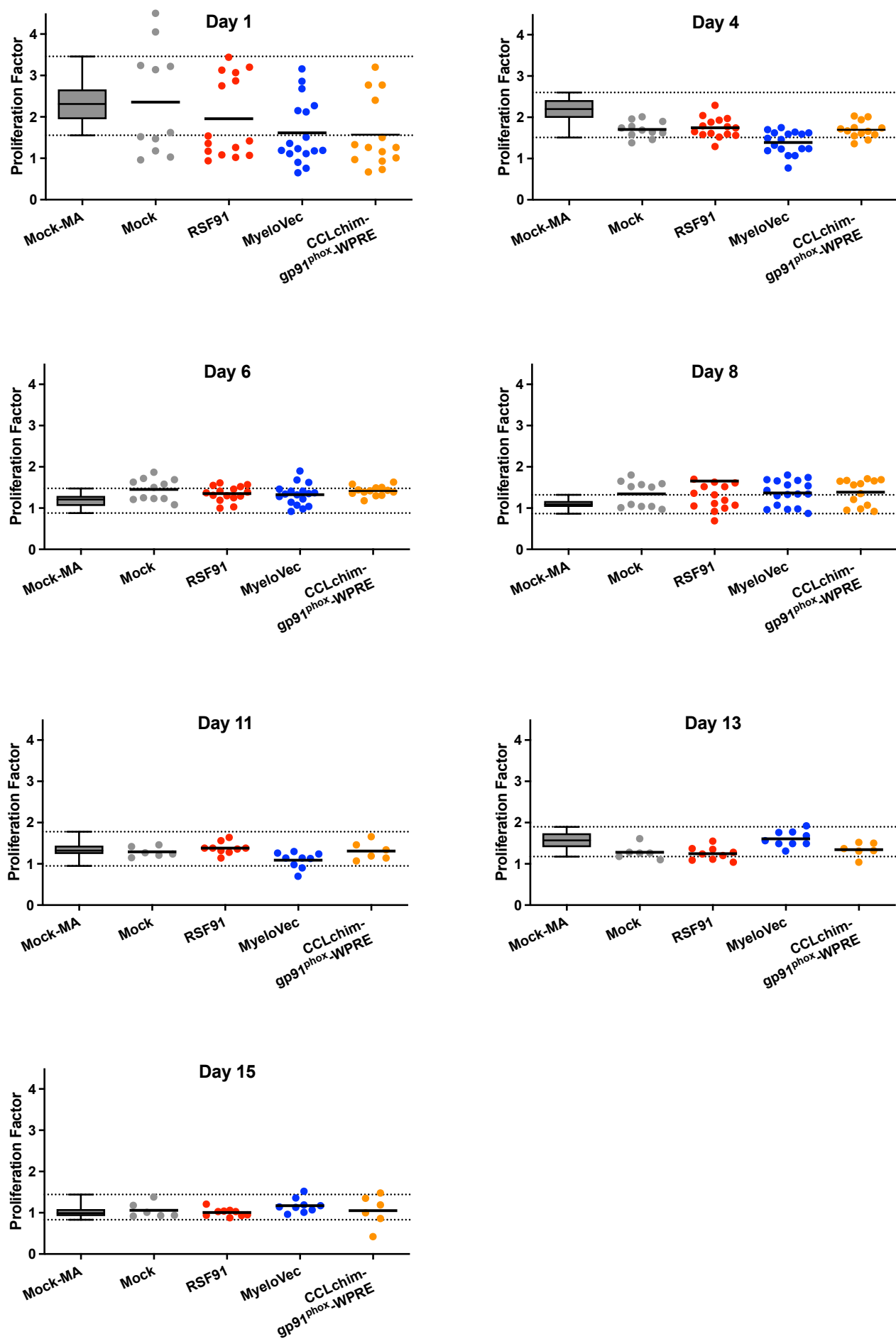


Sup Fig 11) Preservation of MyeloVec Transduced HSPCs in Secondary NBSWG mice

6-7 week old non-conditioned NBSGW mice were transplanted with MyeloVec or mock transduced healthy donor HSPCs. Primary mice were harvested 16-weeks post-transplant and whole bone marrow was pooled from each treatment arm and subsequently transplanted into an equal number of non-conditioned secondary NBSGW mice for an additional 8-weeks. (a) Engraftment of human cells in the bone marrow of the primary and secondary mice are shown. At 8-weeks post secondary transplant, mice were harvested and a portion of the whole bone marrow was FACS sorted to isolate the primitive CD34+ CD38- HSPCs. (b) VCN in the bone marrow of the primary transplanted mice is shown alongside the VCN in the bone marrow and FACS sorted CD34+ CD39- HSPCs in the secondary mice. (c) Lineage distribution of the engrafted human cells are shown in the secondary transplanted mice.

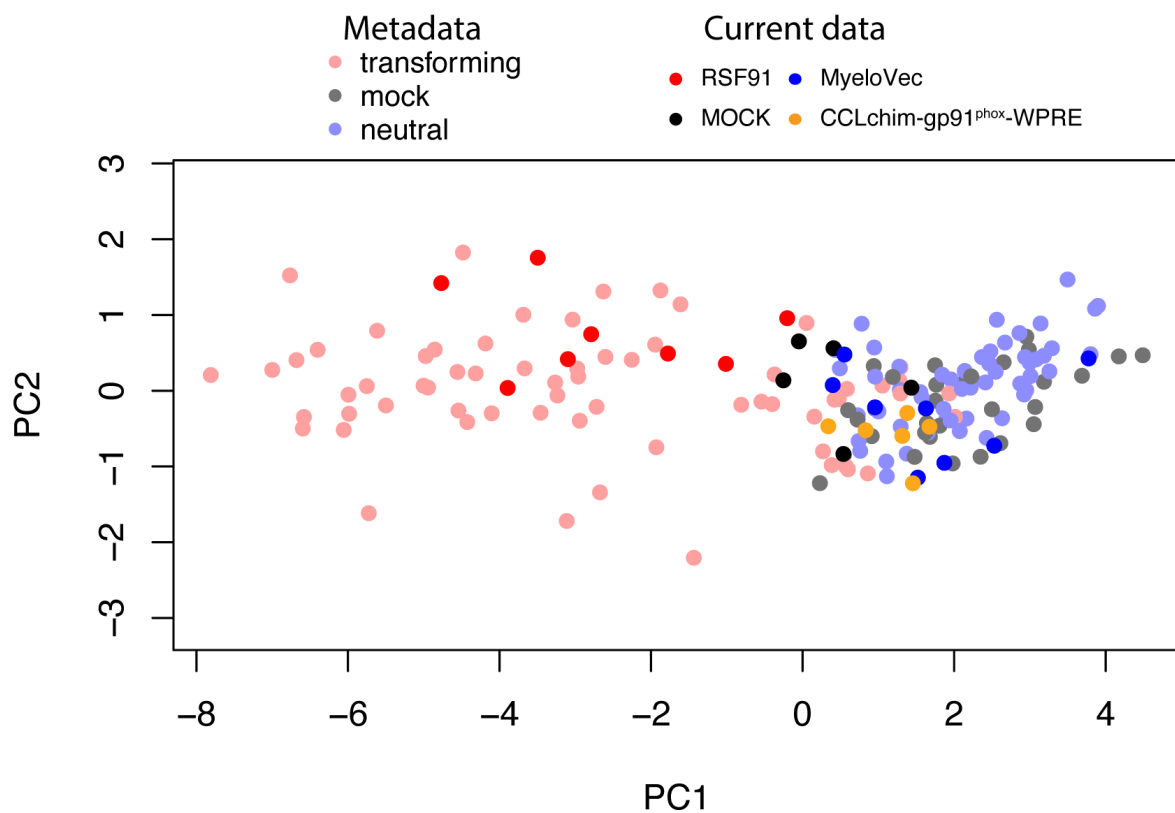
Sup Fig 12) Proliferation rate in IVIM assay and gene clustering in SAGA

a



Sup Fig 12) Proliferation rate in IVIM assay and gene clustering in SAGA

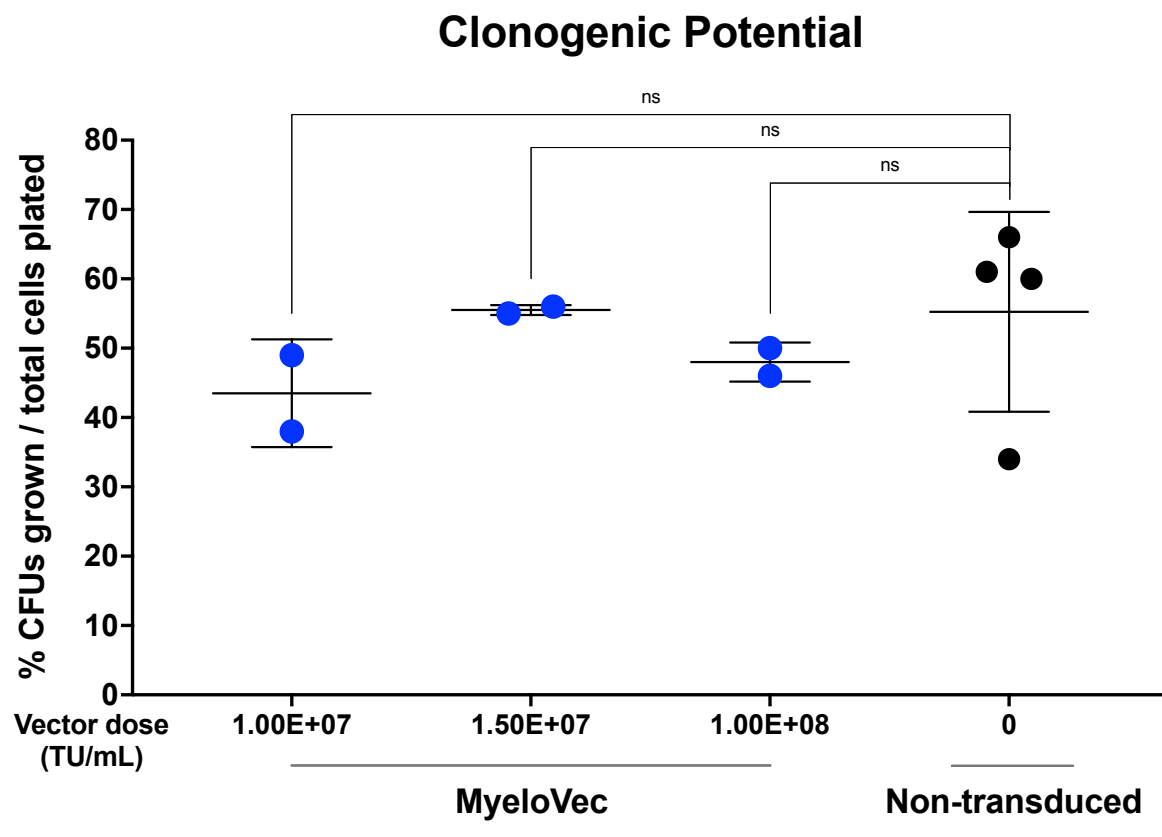
b



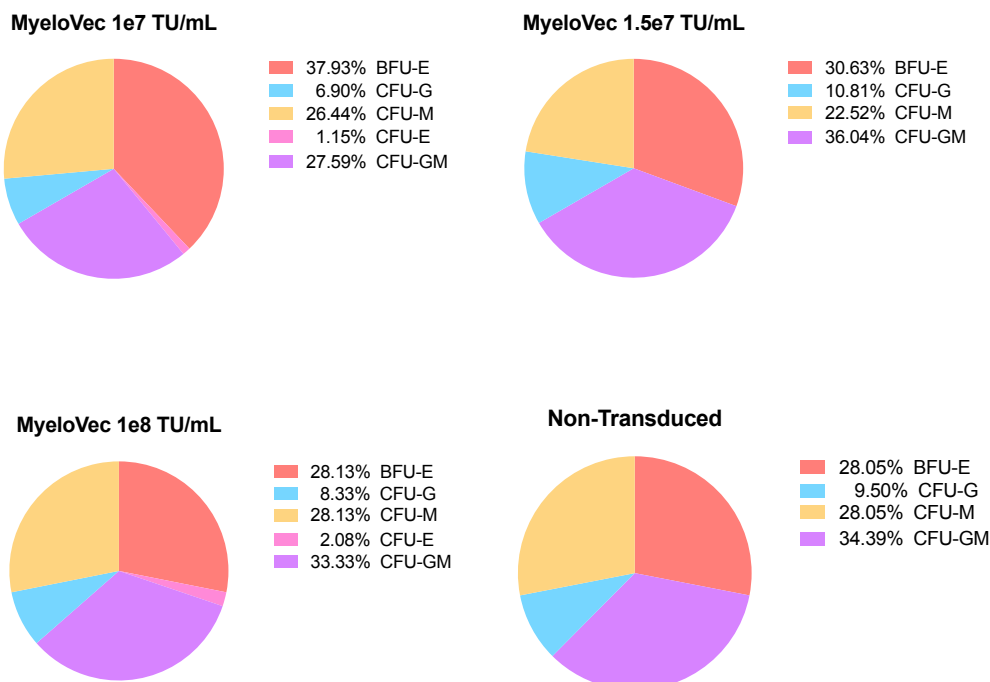
Sup Fig 12) Proliferation rate in IVM assay and gene clustering in SAGA

Dotted lines mark 5% and 95% percentile values of meta-analysis data from 85 Mock controls which are used to determine the expected proliferation rate each day. There were no differences in the proliferation behavior relative to the current mock samples. (b) Principal component plot of gene expression from samples transduced with mutagenic vectors (light red), neutral vectors (light blue), and mock controls from previous assays (light grey). Current samples are depicted in red (RSF91), black (mock), and blue (MyeloVec), or pink (CCLchim-gp91^{phox}-WPRE). Statistical significance was analyzed by Kruskal-Wallis test with Dunn's correction. Bars indicate means.

a



b



Sup Fig 13) Clonogenicity of transduced human hematopoietic stem and progenitor cells.

(a) MyeloVec-transduced healthy donor mobilized peripheral blood HSPCs were assessed for clonogenicity via the colony forming unit (CFU) assay. 100 total cells were plated per replicate. The total number of cells were analyzed after 14 days in culture in methylcellulose-based medium. (b) The distribution of colonies representing the different hematopoietic lineages are shown from each condition. (BFU-E= burst forming unit-erythroid, CFU-G= colony forming unit-granulocyte, CFU-M= colony forming unit-macrophage, CFU-E= colony forming unit-erythroid, CFU-GM= colony forming unit-granulocyte, macrophage). Data are presented as mean \pm SD. Statistical significance was analyzed using an unpaired t-test. All statistical tests were two-tailed and a p value of < 0.05 was deemed significant (ns non-significant, * $P < 0.05$, ** $P < 0.01$, *** $P < 0.001$, **** $P < 0.0001$.)

Sup Table 1) VCN of cell products

14 day <i>in vitro</i> culture of cell products			
	UC-2-4R-Int3-Pro-mCit-WPRE	CCLchim-mCit-WRPE	UBC-mCit-WPRE
Vector concentration (TU/ml)	6.7e6	8.3e6	1.56e7
<i>In vitro</i> VCN	0.96	0.71	0.86
			0.00

Sup Table 2) Sequences of Endogenous Regulatory Elements of *CYBB*

Element	Nucleic Acid Sequence
<i>CYBB</i> Promoter	TAGCACATAAAATTGGCACATATTAAAGCATTGTAAATATCAACCATTACAATTGTTACTACTTTCTCAGCAA GGCTATGAATGCTGTTCCAGCTGTAAAATCACACCTGTTAATGTGTTTACCCAGCACGAAGTCATGTCTA GTTGAGTGGCTAAAAATTGTGATCAAATAGCTGGTAGTTAAAAGTTATTCACTGTGTAACATACATCCCT TAAAATGCACTGTTATTATCTCTAGTTAGAAATTGGTTCACTATGTTAATTGTGACTGGATC ATTATAGACCCCTTTTGAGTTAGGTTAAAGATTAAGTTAGGATGCAAGCTTCACTGTGA CCAATGATTATTAGCCAATTCTGATAAAAGAAAAGGAAACCGATTGCCCAAGGGCTGCTGTTCACTTC ATTGGAAGAAGAACAGCATAGTATAGAAGAAAGGCAAACACAACATTCAACCTCTGCCACC
Minimal <i>CYBB</i> Promoter (core)	TATCTCTAGTTAGAAATTGGTTCACTATGTTAATTGTGACTGGATCATTATAGACCCCTTTTT GTAGTTGTTAGGTTAAAGATTAAGTTAGTTATGGATGCAAGCTTCACTGTGACCAATGATTATTAGCAA TTTCTGATAAAAGAAAAGGAAACCGATTGCCCAAGGGCTGCTGTTCACTTCCTCATTGGAAGAAGAACAT AGTATAGAAGAAAGGCAAACACAACATTCAACCTCTGCCACC
Minimal <i>CYBB</i> Promoter (ultra-core)	TTAAGTTGTTATGGATGCAAGCTTCACTGTGACCAATGATTATTAGCCAATTCTGATAAAAGAAAAGGA AACCGATTGCCCAAGGGCTGCTGTTCACTTCCTCATTGGAAGAAGAACATAGTATAGAAGAAAGGCAA ACAACACATTCAACCTCTGCCACC
Enhancer Element 2	GCTTAGTCATGTTGGTCCAAAGTCATAGTTGATGAGAAGTAGCAAGTTAAGAGAGAAAGACTCTAGAGAT AGGTACATACACAATGATAACAAGTGCACATCAGAGAACCTAAAGGAAGGGCAAAGAAAGAACACTGCAAAG CAGACTCAAACACTAAAGCATAGCAGCTGGGGCAGTTAGTGTAAAGAGAAAAGGAGCTCCATATGCCCTC AATAGAACCTAAGAGCATATTGACTGCATTATTCACTTCACATGTTATTCAACAAATGCTATG TATACTGAGATTTCTGGTCACTGACTGGCTAGAACCTAAAGGAGTGTAGACTATTAAATTAGAGTTACAA TCTGGCAATGATATTAAACAGTCTATTCAAAAAGGGTAACCTCAAGTTAAGCCGGCTAAATGTTATGCAA ATAGGATTTGCCTAAAGTCTAAAGGGTACGAAAAGTGTAGCCATTGAGAATGACTCATTGATGGTGTTC TCGGATGGCTTAAGTATTATTAAATATGTCCTCATTCTAGTGCAGGAACCTCCACGTTTAGAGGAAAGGAGG AAAGAATTGTGAAGACTGTGCTAAAAAAGGTAGAAATTGTTACAATTATTAAAGATAAAAGATAAAGA ACTAGGTTGCTTAAAAAAGGGAGGGAAAGAAAATCAAACATCTTATTGAGGCATTAAAACCTTTAA GAAAATAAATTAAAGTTGATTCTCTAAAATAATTAAACCACTGAAAGTAAATGCA GATTATACTAAGAACACTGTTTACATTCTGCTTCTGAATGGTATTAAAAACTCAGTTATTGAGAAAT GAGGAAGTCTGATCTGCTAGATGAAGGTGGCTGCAGGTGGTATTGCTTATGATGGCAACAAACCG TAAACCCATCACTCAGTAAATTAAACTGGCTGAATGAACTCAAAGCATGTCACATACAGGAAAACACA GCCCTGTTAAGCAGTCTGAAACCCACAAGCTACATGGAAAACACAGATTCAACTACATCATAAAATTCA
Enhancer Element 2 (core)	GAGCTCCATATGCCTCAATAGAACCTAAGAGCATATTGACTGCATTATTCACTTCACATGTTA TTCAACAAATGCTATGTTACTGAGATTTCCTGGTCATTGACTGGCTAGAACCTAAAGGAGTGAGACTAT TAATTAGAGTTACAATCTGGCAATGATATTAAACAGTCTATTCAAAAAGGGTAACCTCAAGTTAAGCCGGCC TAAATGTTATGCAAAATAGGATTTCCTGCTAAAGTCTAAAGGTACGAAAAGTGTAGCCATTGAGAATGAC TCATTTCATGGTGTCTGGATGGCTTAAGTATTATTAAATATGTCCTCATTCTAGTGCAGGAACCTCCACGTT TAGAGGAAAGGAGGAAAGAATTGTGAAGACTGTGCTTAAAAAAGGTAGAAATTGTTACAATTATTAA AGATAAAAGTAAAGAACACTAGGTTGCTTAAAAAAGGGAGGGAAAGAAAATCAAACATCTTATTGAGGC ATTAAAACTTTTAAGAAAATAAAATTAAAGTTGATTCTCTAAAATAATTAAACCACTGAGCTGA AAATGAAAAATGCAGATTACTAAGAACACTGTTTACATTCTGCTTCTGAATGGTATTAAAACCTCAG TTATTTCAGAAATGAGGAAGTCTGATCTGCTAGATGAAGGTGGCTGCAGGTGGTATTGCTTATG TGGCAACAAACCGTAAACCCATCACTCAGTAAATTAAACTGGCTGAATGAATCCAAGCATGTCACATA CAGGAAAAACACAGCCCTGTTAAGCAGTCTGAAACCCACAAGCTACATGGAAAACACAGATTCAACTACATC ATAAAAATTCA
Enhancer Element 2 (ultra-core)	AAATCAAAATACATCTTATTGAGGCATTAAAACCTTTAAGAAAATAAAATTAAAGTTGATTCTC TAAAAATAATTAAACCGCTGAAATGAAAATGCAGATTACTAAGAACACTGTTTACATTCTGC TTTCTGAAATGGTATTAAACCTCAGTTATTCACTGAAATGAGGAGTCTGATCTGCTAGATGAAGGTGGC TGCAGGTGGTATTGCTTATGATGGCAACAAACCGTAAACCCATCACTCAGTAAATTAAACTGGCTG AATGAATCCAAGCATGTCACATACAGGAAAACACAGCCCTGTTAAGCA

Enhancer Element 4	<p>AAACTAATATGACCTTATAAGAGGGAGGAAGTTGGGGCACAGGCATGTACACACAGAGGAAAGACCATAACAG AGGAAAGACCATATTAAGATAAAGGAAGAGGATGACCATCTACAAGCCAAGCAAAGGGGCCAGAAGGA AACCAAACATGCTGAAACCTTGATCTGAATTGTAGCTTCAAAACTGTGAGAAAATAATTCTGTTGTTA AAACATCCAGGCTGAGGTACTTGTATGGAAGCCGTCAAACATAATGCAACAACATTCCCTCATTAGATT TCTTAATTCGTATAGCTGGCCTGATAATGCTTATCAGCTACCCAACTCAATTGCTGCAAATACATTAA AAGTTCTGGTTGAGTTGACACTTGTATGAGCCAATAATGTGAGGCAAGTCTTAAAGGGTA GCACAATCAGTCTGAGGTACACCATAGATATGGTTAACCATAGTGTGGCTCCATAACATAGGAAGTCAAGA TCCCCCTTCACTCTGACCAGTCAGATTGCACCTAGAACATTTCTCAATTGTCATACCACATTAAAGAGGA AGACAAAACCCATGCGTTGTGCAGCTACCACATGTCGAGCATCAGACTATGTGCACTGTGACTACTTAGCTC CCCACCAACCCAAATGAAGATGGTATTAAATACCCACCTCCCATTGTACAGATGAGGAGACTGGGGCTAAATGA GGTCAAATAGGTTGCTCAACAGAGATCTCACCTCCATGGACTCCATGCCACACTCTGAACCCCTGTCATCTC TCAGAAGTGCAGTGCCTCTGAAATCTGCATCTCATACACCCATCCTGACTACCACCTGTTCCCTGGCTTC CTAATTCACTCACACCAAGATGACTGTCTTCACCTCAACCTCATCAAACATTGAGTTCTTGA CTCCCACATCTGTGTTCACTCTGGCATTCTACTCATCTTAGACTCAGTCATTCTGCCATTTCCTGACA CCTGAATTCTCTCATGCAGTGCCTCTGTACCCACCTGCAGGCAAAAACCAACCCGTATCAACTCAATTGCTC CTATACTGCTCGTGGTGGTAAGAAAAGCTAGAAAAGCTACCCACAGACTCTAACCTACATTACTGATT GCTCCAGGCTCAACTGGGCCATTCTGGGCTGGAAATCATTGCAATTCTACAGTCAGTCTCCTTCTGA AAACAGATAACCTGCCCTCTTCAATTCTACAGAGAGGAGGCCCTCTGTCTAAAGCAAATTCCATT GGAAATGGAAACCAACAAAGAGGAAGTCCCTCACCCGCTGTCCCCAGCCCTACAAATCCTCCTGCATCTG TCTGCTCCCTCCCTTTACAGAGAGGAGGCCCTCTGTCTAAAGCAAATTCCATTCTCCTGCCTTGG CTCAGAAATCTCACCCATCCAAATCTCATGGTAGCCTGTCCTTGTGCACTCTTCTCAATT AAGCTCTATATTAAAATAAAACTAGGTCTCTGGTGTTCACATGTGTTCCAATTGTAGCCAAGTC CTCTCATTCTTACACAGCCTCAGACATTGAGGTGTCACTACCTCACCTCAACCCACAACATCTGGCTTCC CTCATTGTTCCAGTAGGCCCTT</p>
Enhancer Element 4R	<p>CAGAGATCTCACCTCCATGGACTCCCATAGCCACACTCTGAACCCCTGTCACTCTCAGAAGTGCAGTCTCT GAAATCTGCATCTCATACACCCATCCTGACTACCACCTCCTGTTCCCTGGCTTCTAATTCACTCACACCCAA GATGACTGTCTTCAACCTCATCAAACATTGAGTTCTTGTACTCTTGA CTTCCTGACTCTTGTCAATTCTCATGCA CTTGGCATTCTACTCATCTTAGACTCAGTCATTCTGCCATTCTGCACAAATCCTGAATTCTCTCATGCA GCTCTCTGTACCCACCTGCAGGCAAAAACCAACCCGTATCAACTCAATTGCTCTTACTTGCTCGTGGG GTAAGAAAAGCTAGAAAAGCTACCCACAGACTCTACCTACTGATTATGAGCTCCAGGCTCAACTGGGCC CTTATCTGGGCTGGAAATCATTGCAATTCTACAGTCAGTCAAGTCTCCTTCTGAACAAAAGATAACACATTGAA AACTGTCTCTGTTCTGAAATGTCTACTCACTACCTCACTTCAACAGATAACCTGCCCTCTTCA GGAAATGGAAACCAACAAAGAGGAAGTCCCTCACCCGCTGTCCCCAGCCCTACAAATCCTCCTGCATCTG TCTGCTCCCTCCCTTTACAGAGAGGAGGCCCTCTGTCTAAAGCAAATTCCATTCTCCTGCCTTGG CTCAGAAATCTCACCCATCCAAATCTCATGGTAGCCTGTCCTTGTGCACTCTTCTCAATT AAGCTCTATATTAAAATAAAACTAGGTCTCTGGTGTTCACATGTGTTCCAATTGTAGCCAAGTC CTCTCATTCTTACACAGCCTCAGACATTGAGGTGTCACTACCTCACCTCAACCCACAACATCTGGCTTCC CTCATTGTTCCAGTAGGCCCTT</p>
Enhancer Element 4R (core)	<p>CATGCAGTGCCTCTGTACCCACCTGCAGGCAAAAACCAACCCGTATCAACTCAATTGCTCTTACTTGCTC GTGGGTGGTAAGAAAAGCTAGAAAAGCTACCCACAGACTCTACCTACTGATTATGAGCTCCAGGCTC AACCTGGCCCTTATCTGGGCTGGAAATCATTGCAATTCTACAGTCAGTCTCCTTCTGAACAAAAGATAAC AACATTGAAAAGCTGCTCTGTTCTGAAATGTCTACTCACTACCTCACTTCAACAGATAACCTGCCCTCTC TTGACAAAGGAAATGGAAACCAACAAAGAGGAAGTCCCTCACCCGCTGTCCCCAGCCCTACAAATCCTCCTG CATCTGCAGTCTGCTCCCTCTTTACAGAGAGGAGGCCCTCTGTCTAAAGCAAATTCCATTCTCCTTCC TGCCCTGGCTCAGAAATCTCACCCATCCAAATCTCATGGTAGCCTGTCCTT</p>
Enhancer Element 4R (ultra-core)	<p>GCCCTTATCTGGGCTGGAAATCATTGCAATTCTACAGTCAGTCAAGTCTCCTTCTGAACAAAAGATAACACATT GAAAAGCTGCTCTGTTCTGAAATGTCTACTCACTACCTCACTTCAACAGATAACCTGCCCTCTTCA AAAGGAAATGGAAACCAACAAAGAGGAAGTCCCTCACCCGCTGTCCCCAGCCCTACAAATCCTCCTGCATCTG CACTCTGCTCCCTCTTTACAGAGAGG</p>

Sup Table 2) Sequences of Endogenous Regulatory Elements of CYBB

Enhancer Element 4L	AAACTAATATGACCTTATAAGAGGGAGGAAGTGGGGCACAGGCATGTACACACAGAGGAAGACCATAACAG AGGAAAGACCATATTAAGATAAAGGAAGAGGATGACCATCTACAAGCCAAGCAAAAGGGGCCAGAAGGA AACCAAACATGCTGAAACCTGATCTGAATTGTAGCTTCTAAAAGTGAGAAAAATAAATTCTGTTGTTA AAACATCCAGGCTGAGGTACTTGTATGGAAGCCCTGTCAAACATAATGCAACAAACATTCCCTCATTAGATT TCTTAATTCTGTATAGCTGGCTGATAATGTCTTATCAGCTACCCAACTCAATTGCTGCAAATACATTTAA AAGTTCTGGTGGTTAGTTGATTGCACACTTCTGTATGAGCCAATAATGTGAGGCAAGTCTTAAAGGGTA GCACAATCAGTCTGAGGTACACCATAGATATGGTTACCCATAGTGTGGTCTCCATAACATAGGAAGTCAGA TCCCCCTTCACTCTTGACCAGTCAGATTGCACCTAGAACATTTCTCAATTCTGCATACCACATTAAAGAGGA AGACAAAACCCATGCGTTGTCAGCTACCACATGTCGAGCATCAGACTATGTGCACTGTGTACACTTAGTCCT CCCACCAACCCATGAAGATGGTATTAATACCCACCTCCATTGTACAGATGAGGAGACTGGGGCTAAATGA GGTCAAATAGGTTGCTAA
Enhancer Element 4L (core)	AGCCAATAATGTGAGGCAAGTCTTAAAAGGGTAGCACAATCAGTCTGAGGTTACCCATAGATATGGTTAA CCATAGTGTGGTCTCCATAACATAGGAAGTCAGATCCCCCTTCACTCTTGACCAGTCAGATTGCACCTAGAA CATTTCTCAATTCTGCATACCACATTAAAGAGGAAGACAAAACCCATGCGTTGTCAGCT
Intron 3 Enhancer	GATCATCCCTCCTGACTTCCATACATGTGGGATTACAGGCATGAGTCACCTGCCTGGCGAGTTCCCTGTTTC TAAGGAGACACAATTCTTTATTCTCCCTACCCCCATTAGAAATAGTTCTATTAGAGGAAGTAAAGCCTGA GAAACAGGCAATGTTTCACCAAGATGGCTGTTAAGAAATCTGGTAGTCTACAAAGTCAAATTCACTGC CGGTGAGCACCATGTCCTGAGCAGCACATGTTGAATGCCAGCTAGAGGTCTCAATCATTGAAACTTGT TTGTAATCCTCTGGTTACCTAGAGAAAGCCCCAGGGTCCCACCCACCACTCCAGGAAAGGTAGG GGTAAAGGCTCTCAGACTGTTGAGAAAAATGGAGAATGGGTGAAGTCAGCACACAAAAATCTGTA GGAAGCCTTAAAAACCCCCACTGCCATGCAGAAACTAATTCTGTCTGGATGGCAGTCAGTCTTAAGAT CAGAAAGAAACAGGAAGGTGAGAGGGTGAGGTTATCTTACCTTATATAGTCTGGAGTCAGAGGCAC TCAGTGTGCCTCTATTTAATCACGTGGCTAGCACTAGTCTCTGGCTTCTGCTCATAGTTTTTTTA GTTGAAAAACAGGTCAACTAACACAAATGTAAGAAGGCATATGTTGCTAAAAGTATATTAAATTGTTAAAGT CTGTCATTAGTGTGAGTTGTCAGTCATAAAATATTGTTGAGTGCCTATGTGCTAACGACTGGGGACATGT GGTAAGTAAAGATTAAGTTAGATAGGCCATGAGCTTAAGGAGCTAGAGTGTAAACAGGAGAGACAGAG AATAAAATGGAACCTCCAAATTATAACAGTGTATGCAAATAAGGTAGTGTATTATCATATTATCAGATATT CTACTGCCAGCAGGTGTGGATATTACTGTCAACTTACTGCCCTGAGTTCTGTAGATTCAAAGTGGATTGTA ATTCTCCAGTTGCGTATAAAATCTAAATCAGACATATTGATGGTGCCTGTTGAGATCAAGTGTACAAA AAGTAGAGCTTGTGAGTTCTGTAAGTGTACACCCCCATAAAATATGTAATTCTTTAGTCCACTCCCTT TTCTGAAATATTCTTACTCAGTTCAATAGACATAGAAATCTGCTGAAGTGTACTCAATAATCTCCCTT GCATTAGAATGGTAGTTATTGAAATCGGGCAAGGCTCCGGTACAGTAACAGAGAAACTCCCTTAGAA GTCAATGGCAGAAAGTAAGTAGTAAGGAAGCTATGGGGCATGATGGCAACGTGGATAATTGGGAA GTGGCTGGCAATAATTAGAAGTAACGATATAATGCAATCTGCCCTGATGATGGGAACAAAAAAT TATGGGCAGTCACAGACAGTAAAGTCTCTTCTATGCCACCAACGGGTGCTCGCCTCTTTAAGGA AGTGGTGAGGAGATGGTATTCTAAAGCCAGTATCAGCATGACTTGTGGCTTCTTTGGATTGTTGCC ATTCTGTCCACACCAAGAGGGTAGGTGGAAAAATTAGGGATTGTGCCCTGATGGTGGACCCACTCCA CTGATCCATTAGTTACTAGTAATCTCACTTTCTCAATATAATATGTGTTTACATTAACAGCTTTTA AAAATTACCTATTAAGATGAAA

Sup Table 2) Sequences of Endogenous Regulatory Elements of CYBB

Sup Table 2) Sequences of Endogenous Regulatory Elements of *CYBB*

Sup Table 2) Sequences of Endogenous Regulatory Elements of *CYBB*

GeneArt codon optimized gp91 ^{phox}	ATGGGAAACTGGGCCGTGAATGAGGGCCTGAGCATCTCGTGTGGCTGGGCTGAACGTGTC CTGTCGTGTTACTACCGGGTGTACGACATCCCTCTAACGTTCTACACCCGGAAGCTGCTGGGCTCTG CTCTGGCTTGTAGAGCACCAAGCCCTGCCTGAACCTCAACTGCATGCTGATCCGTGCTGCCGTGCG GAACCTGCTGAGCTTCTGAGAGGCAGCAGCGCCTGCTGAGCACAGAGTTAGACGGCAGCTGGACAGAA ACCTGACCTTCCACAAGATGGTGGCTGGATGATGCCCTGCACAGGCCATTACACAAATGCCACCTGTT CAACGTCGAGTGGTGCCTAACGCCAGAGTGAACAACAGCAGCCATTACAGCGTGGCCGTGAGCGAGCTGG GCGATAGACAGAATGAGAGCTACCTGAATTGCCCGGAAGCGGATCAAGAACCTGAAGGCGGACTGTAC CTGGCGTGTGACTGCTGGCTGGAATCACAGCGTGGTCATCACCCTGTGCTGATCCGTGATCATCACCGCA GCACCAAGACCATCCGGCGGAGCTACTCGAGGTGTTCTGGTACACCCACCACTGTTGTGATCTTTTCATC GGCCTGGCCATCCACGGCGCCGAGAGAATCGTAGAGGACAGACAGCCAGTCTGGCCGTGACAATAT CACCCTGCGAGCAGAAAATCAGCGAGTGGGCAAGATCAAAGAGTGCCCCATTCTCAGTTGCCGGCA ATCCTCTATGACCTGGAAGTGGATCGTGGGCCCATGTTCTGTACCTGTGCGAAAGACTCGTGCAGGTTCTG GCGGAGGCCAGCAGAAGTGGTCATTACCAAGGTGCTGACACACCCCTTAAGACCATCGAGCTGCAGATGAA GAAAAAGGGCTCAAGATGGAAGTGGCCAGTACATCTTGTGAAGTGCCCCAAGGTGTCAGCTGGAAT GGCACCCCTTCACACTGACAAGGCCCTGAAGAGGACTCTTCAGCATCCACATCCGGATGTCGGCGATTG GACCGAGGGCCTGTTAATGCCCTGCGCTGCGACAAGCAAGAGTCCAGGATGCTGGAAGCTGCCAAGAT CGCCGTGGACGCCCTTGGAACAGCCAGCGAGGACGTTAGCTACGAGGTGCTGATGTCGTTGAG CCGGCATCGGCGTGCACACCTTGGCAGCATCCTGAAGTCTGTGTTGACAAGTACTGCAACAAACGCCACCAA CCTGAAGCTCAAGAAGATCTACTTCACTGGCTGCGGGACACCCACGCCCTTGAGCTACAACATCTACCTGACC CTGCAGCTGCTGAAAGCCAGATGCAAGAGAGAAACAAGGCCGCTCTGAGCTACAACATCTACCTGACC GGCTGGGATGAGAGGCCAGGCAATCACTTGCGCTGCAACCGACGAAGAGAAGGACGTGATCACCAGCCT GAAGCAGAAAACCCCTGTACGGCAGACCCAACGGAGTTCAAGACAATGCCCTCTAGCACCCCCAA TACCAAGATCGGAGTGTGTTCTGTGCGGCCCTGAGGCTCTGGCCGAAACACTGAGCAAGCAGACATCAGCAA CAGCGAGTCTGCCCTAGAGGCGTGCACCTCATCTCAACAAAGAGAACCTCTGA
IDT codon optimized gp91 ^{phox}	ATGGGTAACTGGGAGTGAACGAGGGGCTTCTATCTTGTCTACTCGTGTGGCTGGCCTAACGTGTTCT TGTCGTCTGGTACTACCGAGTGTACGACATTCCCTCTAAATTCTTACACACGCCAAACTCTTGGGCTGCTT TGGCGCTCGCTCGGGCACCTGCAGCGTGCCTGAATTAACTGTATGCTGATCTCTCTGTGCGCCGAAA CCTCTTTCATTCTCGAGGTAGTCCGCTGCTCAACTCGGGTGCAGCGAGCTGACCGCAACCTG ACGTTCCATAAGATGGTAGCATGGATGATTGCGTTGCATTCCCGATCCACACTATCGCGCACCTTTAACG TGGAAATGGTGTAAACCGAGAGTAAATAACAGCAGCCATACTCTGAGCTACCTCCGAACCTGGAGACC GGCAGAACGAATCTACCTAACCTGCTAGGAAGAGAATTAAAAACCCAGAAGGTGGCCTTATCTCGCG TTACGCTGCTGCTGGCATTACCGGCGTTGTCATAACTCTGTTGATACTTATAATTACAAGCTCCACCAAG ACTATAAGACGATCCTACTTGAAGTCTCTGGTACACGCAACACCTGTTGTAATTCTTATAAGGACTGGC TATTCACTGCTGGCAGACAGCTGAGCTGAGGATTGAGCTGAGGATGAGCTGAGGATGAGCTGAGGATGAG CGAGCAGAACGATAAGTGAAGTGGGGAAAAATTAAAGAGTGGCCCATACACAGCTGAGGATGAGCTGAGG TGACATGGAAAGTGGATCGTGGGCCCATGTTCTACCTGTGAGCGCCTGTAAGGTTGGCGAACGCC AACAGAAAAGTAGTGATAACGAAAGTAGTTACACACCCGTTCAAGACAATAGAGCTCCAGATGAAAAAAA GGCTCTAACGAGATGGAAAGTCGGTCAATACATATTGAGCTGAGGATGAGCTGAGGATGAGCTGAGG TTCACTCTCACATCAGCGCTGAAGAAGACTTTCTCCATTCAATTGAGCTGAGGATGAGCTGAGG GGCTCTAACGAGATGGAAAGTCGGTCAATACATATTGAGCTGAGGATGAGCTGAGGATGAGCTGAGG ATGGGCCGTTGGAACCGCCAGCGAAGATGTTGAGCTGAGGATGAGCTGAGGATGAGCTGAGG GAGTTACTCCGTTGCTCCATACTTAAGAGCGTCTGGTACAAATATTGTAATAATGCCACCAATTGAAACTC AAGAAGATTACTTTATTGGTTGTAGGGACTACGCTTCAATGGTCTGAGCAGACCTCCAGCTCCT TGAAAGCCAATGCAGGAACGAAATAACCGCAGGATTTGAGCTACAATATACCTACGGGTTGGGACGA ATCTCAGGCTAATCATTCCGGTACACCATGATGAGAAAAGGATGTTATAACGGGTTGAAACAAAAAC ACTCTATGGACGACCTAACGGATAATGAAATTAAAACATGCCAGCCAACATCTAACACCCGGATTGGA GTTTCCCTGTGCGGGCCAGAGGCACTCGCGAGACGCTGAGTAAACAATCAATTAGCAACTCTGAGTCCGGG CCACGCGGGGTGCACTTTATTAAACAAAGAGAACCTCTAG

Supplemental Materials and Methods:

Generating the Lead Candidate Vector

Further analysis revealed element 4 consisted of two distinct 749bp (left) and 955 (right) fragments (Sup Fig 3a). We demonstrated that only the right fragment was necessary for expression, allowing removal of 749 bp of inert sequence (Sup Fig 3c-f). To design our composite candidate vector, we combined the B cell specific enhancer (element 2) with the right fragment of the myeloid specific enhancer (element 4R) (Sup Fig 3).

Optimizing the Lead Candidate Vector Improves Expression, Titer and Gene Transfer

We have previously observed a negative correlation between proviral size in relation to viral titer and gene transfer^{1,2}. Therefore, we set out to further decrease the size of each enhancer element within the composite vector to increase titer and gene transfer while maintaining expression. Using ENCODE³ data to define the minimal functional boundaries of each element, we generated new, smaller variants termed “core” and “ultra-core” (UC) (Sup Fig 4a). We re-screened composite vectors containing the core and UC variants in CB CD34+ differentiated neutrophils and monocytes and in Jurkat and RAMOS cells (Sup Fig 5). The core variant, containing 1182 bp of deletions, decreased expression by 15% in mature neutrophils compared to the parental vector (2-4R-Int3) (Sup Fig 5a). While the UC variant, containing 2882 bp of deletions, increased expression in neutrophils by 1.8-fold compared to the parental vector. Similar results were observed in the monocytes and in RAMOS cells with the UC variant expressing 1.5-fold and 1.2-fold higher than the parental vector, respectively (Sup Fig 5b-c). Meanwhile, the core variant decreased expression by 33% in monocytes and 6% in RAMOS cells. In addition to increasing expression in the on-target cellular populations, the UC variant retained lineage specific expression with no off-target expression detected in Jurkat T cells (Sup Fig 5d).

As expected, introducing a series of deletions to decrease proviral length resulted in a gradual increase in titer with the UC variant having a 3.3-fold higher titer compared to the parental vector (Sup Fig 5e). We also observed a correlation between decreased proviral size and increased gene transfer in human BM CD34+ HSPCs (Sup Fig 5f). At a vector dose of 1×10^8 transduction units (TU)/mL, the UC variant had a 10-fold higher gene transfer than the parental vector, producing an average stable VCN of 3.76 compared to 0.35, respectively. By introducing a series of systematic deletions to decrease proviral length, we generated our lead candidate vector - MyeloVec (UC variant of 2-4R-Int3-pro-mCit-WPRE), with improved titer, gene transfer, and expression.

Supplemental Methods:

Murine X-CGD HSPCs into Pepboy Secondary Transplants:

Primary mice were harvested 16-weeks post-transplant and whole bone marrow was collected and pooled from each treatment arm. $30e^6$ whole bone marrow cells were injected retro-orbitally into each of the lethally irradiated secondary Pepboy recipients. Secondary transplanted mice were harvest after an additional 16-weeks.

HD HSPCs into NBSGW Secondary Transplants:

6-7 week-old non-conditioned NBSGW mice were transplanted with 0.8-1.8e6 MyeloVec or mock transduced HD HSPCs. At 16-weeks post-transplant, primary NSBWG were harvested and whole BM was pooled from each treatment arm and transplanted into an equal number of non-conditioned NBSGW secondary mice for an additional 8-weeks. CD34+ CD38- HSPCs were FACS sorted from the BM of the secondary mice for VCN analysis.

Lentiviral vector transduction:

Human CD34+ cells were plated on retronectin (Takara Shuzo)-coated (20 ug/ml) plates with X-VIVO15 (Lonza Biosciences) supplemented with 1X Penicillin-Streptomycin-Glutamine (P/S/G), and 50 ng/mL each of human stem cell factor (hSCF), human thrombopoietin (hTPO), and human FMS-like tyrosine kinase 3 ligand (hFlt3-L), and 20 ng/mL of human interleukin-3 (hIL3) for 24 hours pre-stimulation before lentiviral transduction for 24 hours. For cells to be xenografted into mice, hIL-3 was excluded from the pre-stimulation media. For transduction of X-CGD patient cells, 1mg/mL poloxamer synperonic F108 (Kolliphor P338; BASF, Ludwigshafen, Germany) and 10uM prostaglandin E2 (PGE2) was added for 24hrs during lentiviral transduction.

For transduction of murine Lin- HSPCs, pelvis, femur, and tibia-derived BM cells of B6.129S6-Cybb^{tm1Din/J} or C57BL/6J mice were isolated using the Miltenyi Direct Lineage Depletion Kit (Miltenyi Biotec). Lin- cells were plated on retronectin-coated plates and cultured in StemSpan SFEMII (Stem Cell Technologies) supplemented with 1X P/S/G, 100 ng/mL of murine TPO, and 10 ng/mL of murine SCF with lentiviral supernatant for 24 hours.

PLB-985, Jurkat and RAMOS cell lines were transduced with LV supernatant in culture media for 24 hours at a range of concentrations to achieve an equivalent vector copy number (VCN).

DHR and Cytochrome C assays:

Restoration of oxidase activity was measured by the Dihydrorhodamine (DHR) and Cytochrome C assays as previously described⁴.

Determination of VCN by digital droplet PCR (ddPCR):

Genomic DNA was extracted using PureLink genomic DNA kit (Invitrogen) and average VCN per cell was measure by ddPCR as previously described⁵.

Colony Forming Unit (CFU) assay:

100 HSPCs per replicate were plated in MethoCult (StemCell Technologies H4434) 24 hours after LV transduction. The number of mature colonies were counted and scored under microscope based on their specific morphology after 14 days in culture.

Cell culture:

To induce human neutrophil differentiation, transduced or unmodified umbilical CB or BM CD34+ cells were collected and cultured in StemSpan SFEM II (Stem Cell Technologies) supplemented with 10% fetal bovine serum (FBS) (Gemini Bio), 1X Penicillin-Streptomycin-Glutamine (P/S/G) (Gemini Bio), and 100 ng/mL human stem cell factor (hSCF), 100 ng/mL human thrombopoietin (hTPO), 10 ng/mL human granulocyte colony stimulating factor (hGSCF), and 10 ng/mL of human Interleukin 3 (hIL3) for 7 days (PeproTech). For the final stages of neutrophil differentiation, cells were collected and re-cultured in StemSpan SFEM II with 10% FBS, 1X P/S/G, and 10 ng/mL hGSCF for an additional 7-11 days. To verify successful neutrophil differentiation, polynuclear morphology of cells were confirmed by Wright-Giemsa staining.

Human monocyte differentiation conditions were adapted from a previously established protocol⁶. Briefly, transduced or unmodified CB CD34+ cells were cultured in X-VIVO 15 (Lonza Bioscience) supplemented with 10% FBS, 1X P/S/G, 50 ng/mL of hSCF, 15 ng/mL hTPO, 30 ng/mL hIL3, and 30 ng/mL of human Flt3-ligand (hFlt3L) for 9 days. Cells were then collected and re-cultured in StemSpan II with 20% FBS, 1X P/S/G, 25 ng/mL hSCF, 30 ng/mL human macrophage colony stimulating factor (M-CSF), 30 ng/mL hIL3, and 30 ng/mL hFlt3L for an additional 7 days.

The human PLB985 *CYBB*^{-/-} cell line was kindly provided by Dr. Adrian J. Thrasher. The PLB985, Jurkat and RAMOS cell lines were cultured in Roswell Park Memorial Institute (RPMI) -1640 media (Corning) supplemented with 10% FBS and 1X P/S/G.

Neutrophils were differentiated from murine Lin- cells as previously described⁷. Briefly, transduced or unmodified murine Lin- cells were cultured in Iscove's Modified Dulbecco's Medium (IMDM) (Gibco) with 20% FBS and 1X P/S/G, supplemented with 50 ng/mL murine SCF and 50 ng/mL murine IL3 for 3 days. In the following 2 days, the media was supplemented with 50 ng/mL murine SCF, 50 ng/mL murine IL3, and 50 ng/mL human GCSF. Cells were then transferred to media supplemented with 50 ng/mL human GCSF alone for an additional 7 days in culture.

For gene transfer evaluations at various LV transduction doses, we cultured transduced murine Lin- cells in murine basal bone marrow media (BBMM) comprised of StemSpan SFEM II, 1X P/S/G, 50 ng/mL murine SCF, 20 ng/mL IL3, and 50 ng/mL human Flt3-L for 14 days.

FACS analysis:

For detection of gp91^{phox} in different cellular lineages of HD BM and PB samples, cells were co-stained with anti-human CD45-APC (HI30), CD33-V421 (WM53), CD3-PerCp-Cy5.5 (UCHT1), CD19-PE-Cy7 (SJ25CI), CD34-APC-Cy7 (581), CD90-BV605 (5E10), CD38-BV711 (HIT2), and gp91^{phox}-FITC (7D5) antibodies. All antibodies above were purchased from BD Biosciences with the exception of CD38-BV711 and gp91^{phox}-FITC which were purchased from Biolegend and Lifespan Biosciences, respectively. For detection of gp91^{phox} in the various stages of neutrophil development, cells were co-stained with CD16-APC-Cy7 (B73.1), CD66b-APC (G10F5), CD11b-PE (ICRF44), CD15-V450 (H198), CD14-PE-Cy7 (63D3), and gp91^{phox}-FITC (7D5). All neutrophil antibodies were purchased from Biolegend except for CD15-V450 (BD Biosciences).

To measure expression of mCitrine across the different cellular lineages in the BM, spleen, and PB of NSG mice transplanted with human CB CD34+ HSPCs, cells were co-stained with the aforementioned lineage and neutrophil antibodies. To detect mCitrine in human CD34+ differentiated neutrophil and monocytes, cells were co-stained with the neutrophil antibodies listed above.

For detection of gp91^{phox} *in vitro*, differentiated neutrophils from murine Lin- cells were stained with anti-mouse Ly-6G-PE (1A8) and CD11b-APC (M1/70), along with anti-human gp91^{phox}-FITC (7D5).

To measure restoration of gp91^{phox} across the different lineages of Pepboy mice transplanted with either murine X-CGD or WT cells, BM and PB samples were co-stained with anti-mouse Gr1-V450 (RB6-8C5), Ly6A/E-BV711 (D7), CD117-BV786 (2B8), CD45.2-PerCp-Cy5.5 (104), CD3-PE (172A), CD45.1-PE-Cy7 (A20), CD11b-APC (M1/70), and CD45R-APC-Cy7 (RA3-6B2) along with anti-human gp91^{phox}-FITC (7D5). All murine lineage antibodies were purchased from BD Biosciences.

Ghost Violet 510 viability dye (Tonbo Biosciences) was also added to all samples. Samples were analyzed on either a LSRII or LSR Fortessa flow cytometer (BD Biosciences).

Visual Abstract:

The visual abstract was created with BioRender.com

Supplemental References:

1. Morgan RA, Unti MJ, Aleshe B, et al. Improved Titer and Gene Transfer by Lentiviral Vectors Using Novel, Small β -Globin Locus Control Region Elements. *Mol. Ther.* 2019;28(1):328–340.
2. Han J, Tam K, Ma F, et al. β -Globin Lentiviral Vectors Have Reduced Titers due to Incomplete Vector RNA Genomes and Lowered Virion Production. *Stem Cell Reports.* 2020;16(2020):1–14.
3. Dunham I, Kundaje A, Aldred SF, et al. An integrated encyclopedia of DNA elements in the human genome. *Nature.* 2012;489(7414):57–74.
4. Santilli G, Almarza E, Brendel C, et al. Biochemical correction of X-CGD by a novel chimeric promoter regulating high levels of transgene expression in myeloid cells. *Mol. Ther.* 2011;19(1):122–132.
5. Masiuk KE, Laborada J, Roncarolo MG, et al. Lentiviral Gene Therapy in HSCs Restores Lineage-Specific Foxp3 Expression and Suppresses Autoimmunity in a Mouse Model of IPEX Syndrome Short Article Lentiviral Gene Therapy in HSCs Restores Lineage-Specific Foxp3 Expression and Suppresses Autoimmunity. *Cell Stem Cell.* 2019;24(2):309-317.e7.
6. Stec M, Weglarczyk K, Baran J, et al. Expansion and differentiation of CD14+CD16 and CD14++CD16+ human monocyte subsets from cord blood CD34+ hematopoietic progenitors. *J. Leukoc. Biol.* 2007;82(3):594–602.
7. Gupta D, Shah HP, Malu K, Berliner N, Gaines P. Differentiation and Characterization of Myeloid Cells. *Curr Protoc Immunol.* 2014;104 (1) 22F.5.1-22F.5.28.